

RESEARCH ARTICLE

Marine biodiversity at the end of the world: Cape Horn and Diego Ramírez islands

Alan M. Friedlander^{1,2*}, Enric Ballesteros³, Tom W. Bell⁴, Jonatha Giddens², Brad Henning⁵, Mathias Hüne⁶, Alex Muñoz¹, Pelayo Salinas-de-León^{1,7}, Enric Sala¹

1 Pristine Seas, National Geographic Society, Washington DC, United States of America, **2** Fisheries Ecology Research Laboratory, University of Hawai'i, Honolulu, Hawai'i, United States of America, **3** Centre d'Estudis Avançats (CEAB-CSIC), Blanes, Spain, **4** Department of Geography, University of California Los Angeles, Los Angeles, California, United States of America, **5** Remote Imaging Team, National Geographic Society, Washington DC, United States of America, **6** Fundación Ictiológica, Santiago, Chile, **7** Charles Darwin Research Station, Puerto Ayora, Galápagos Islands, Ecuador

* alan.friedlander@hawaii.edu



Abstract

The vast and complex coast of the Magellan Region of extreme southern Chile possesses a diversity of habitats including fjords, deep channels, and extensive kelp forests, with a unique mix of temperate and sub-Antarctic species. The Cape Horn and Diego Ramírez archipelagos are the most southerly locations in the Americas, with the southernmost kelp forests, and some of the least explored places on earth. The giant kelp *Macrocystis pyrifera* plays a key role in structuring the ecological communities of the entire region, with the large brown seaweed *Lessonia* spp. forming dense understories. Kelp densities were highest around Cape Horn, followed by Diego Ramírez, and lowest within the fjord region of Francisco Coloane Marine Park (mean canopy densities of 2.51 kg m⁻², 2.29 kg m⁻², and 2.14 kg m⁻², respectively). There were clear differences in marine communities among these sub-regions, with the lowest diversity in the fjords. We observed 18 species of nearshore fishes, with average species richness nearly 50% higher at Diego Ramírez compared with Cape Horn and Francisco Coloane. The number of individual fishes was nearly 10 times higher at Diego Ramírez and 4 times higher at Cape Horn compared with the fjords. Drop-cam surveys of mesophotic depths (53–105 m) identified 30 taxa from 25 families, 15 classes, and 7 phyla. While much of these deeper habitats consisted of soft sediment and cobble, in rocky habitats, echinoderms, mollusks, bryozoans, and sponges were common. The southern hagfish (*Myxine australis*) was the most frequently encountered of the deep-sea fishes (50% of deployments), and while the Fuegian sprat (*Sprattus fuegensis*) was the most abundant fish species, its distribution was patchy. The Cape Horn and Diego Ramírez archipelagos represent some of the last intact sub-Antarctic ecosystems remaining and a recently declared large protected area will help ensure the health of this unique region.

OPEN ACCESS

Citation: Friedlander AM, Ballesteros E, Bell TW, Giddens J, Henning B, Hüne M, et al. (2018) Marine biodiversity at the end of the world: Cape Horn and Diego Ramírez islands. PLoS ONE 13(1): e0189930. <https://doi.org/10.1371/journal.pone.0189930>

Editor: Giacomo Bernardi, University of California Santa Cruz, UNITED STATES

Received: October 2, 2017

Accepted: December 5, 2017

Published: January 24, 2018

Copyright: © 2018 Friedlander et al. This is an open access article distributed under the terms of the [Creative Commons Attribution License](https://creativecommons.org/licenses/by/4.0/), which permits unrestricted use, distribution, and reproduction in any medium, provided the original author and source are credited.

Data Availability Statement: All data are available within the paper, its Supporting Information files, and at Dryad: doi:[10.5061/dryad.jf36b](https://doi.org/10.5061/dryad.jf36b).

Funding: We received funding from The Brooks Foundation, The Keith Campbell Foundation for the Environment, The Case Foundation, Leonardo DiCaprio Foundation, Davidoff, The Don Quixote Foundation, Roger and Rosemary Enrico Foundation, Helmsley Charitable Trust, Lindblad Expeditions-National Geographic Fund, Philip Stephenson Foundation, Vicki and Roger Sant, The

Waite Foundation, and The National Geographic Society. The funders had no role in study design, data collection and analysis, decision to publish, or preparation of the manuscript.

Competing interests: We received funding from commercial sources: National Geographic Society, Davidoff, and Lindblad Expeditions. The funders had no role in study design, data collection and analysis, decision to publish, or preparation of the manuscript. This does not alter our adherence to PLOS ONE policies on sharing data and materials.

Introduction

Kelp forests are the foundation of many of the shallow rocky coasts of the world's cold-water marine habitats, providing food and three-dimensional structure for a wide range of species [1–4]. They produce the largest biogenic structures in the ocean, are important in marine carbon cycles, and constitute one of the most diverse and productive ecosystems on the planet [5–8]. Kelp forests are important recruitment and nursery habitat for numerous species and provide a key link between nearshore and deep-water habitats [2,4,9]. The biomass and persistence of these kelp forests are controlled by many biotic and abiotic factors including disturbance from large wave events, seasonal and interannual nutrient inputs, top-down consumer interactions, and anthropogenic degradation of habitat [10–15]. The relative impacts of these forces are often difficult to tease apart since there have been major reductions in kelp forest community biodiversity over the past few centuries, leading to a lack of understanding of what the natural community was like in the past [16–19].

The vast and complex Magellan Region of extreme southern Chile consists of a diversity of habitats including fjords, deep channels, inland seas, glaciers, and extensive kelp forests that are the product of glacial and post-glacial processes [20], which have created remarkably high levels of terrestrial endemism and the largest temperate forests in the Southern Hemisphere [21–23]. The region still contains largely unfragmented ecosystems, low anthropogenic impacts, and very low population density [23].

The Magellan Region contains the archipelago of Tierra del Fuego, with the main island—Isla Grande de Tierra del Fuego—and numerous smaller islands, including the Cape Horn and Diego Ramírez archipelagos [24–25]. This region is the confluence of water masses from three great oceans (Pacific, Atlantic, and Southern oceans), with a mix of species of temperate and sub-Antarctic distributions that creates a unique area of marine endemism with high biodiversity value [26–27]. The region contains critical habitats for marine mammals of global conservation concern (e.g., humpback whales *Megaptera novaeangliae*, southern right whale *Eubalaena australis*) [28–29], and a number of Important Bird and Biodiversity Areas (IBA) [30–31].

The indigenous Yaghan people, noted by Darwin during the voyage of the Beagle [32], were hunters and gatherers who settled the region ~ 10,000 years ago, and represent the world's southernmost ethnic group [33–35]. Today only 2,200 people live in the Magellan region, most of them in Puerto Williams, which is located on Navarino Island in the Beagle Channel and is the southernmost town in the world [36]. The Patagonian toothfish (*Dissostichus eleginoides*) and southern hake (*Merluccius australis*) fisheries were once important to the economy of the region, but severe overfishing in recent years has greatly reduced the catch of these species [37–38]. The southern king crab (*Lithodes santolla*) and false king crab (*Paralomis granulosa*) fisheries are currently the most important economic activities in the region, but large declines have recently been noted for these species as well [36].

The marine ecosystems of the Magellan Region are diverse with unique biogeography, yet have been poorly studied to date [39]. The region possesses the southernmost kelp forests in the world and therefore has extremely high biodiversity value. The importance of these shallow water habitats as nurseries for commercially valuable resource species and the interconnectivity among deep and shallow habitats is largely unknown. The vast expanses of unfragmented habitats within the region have been recognized for their pristine condition, but efforts to maintain this healthy ecological state are challenged by a variety of human impacts including: overfishing, aquaculture, tourism, transportation, and insufficient management capacity [36,40]. With these factors in mind, we set out to conduct a comprehensive and integrated assessment of the marine ecosystems of the region to: 1) compare the marine communities

under different environmental regimes, 2) establish baselines for future comparisons, 3) conduct the first marine assessment of Diego Ramírez, and 4) help inform management of this unique region, including the potential benefits of increased protection.

Methods

Ethics statement

Data were collected by all authors in a collaborative effort. Field work and fish collection permits were granted by the Chilean Fisheries Service under a Technical Memorandum (P.INV N° 224/2016 SUBPESCA). This study was carried out in strict accordance with the recommendations of the Canadian Council on Animal Care guidelines on euthanasia of animals used in science. Animal Care and Use was approved by the Charles Darwin Foundation Animal Care and Use Committee under permit number 2017–002. Fish were euthanized using clove oil prior to preservation, and all efforts were made to minimize suffering. Our data are available at Data Dryad: doi:[10.5061/dryad.jf36b](https://doi.org/10.5061/dryad.jf36b).

Site descriptions

Francisco Coloane Marine Park is located within the western portions of the Straits of Magellan between Santa Inés and Riesco islands and the Brunswick Peninsula, and includes Carlos III Island (Fig 1). The park, established in 2003, was the first marine national park in Chile, and was specifically designated to conserve feeding areas for humpback whales and breeding areas for Magellanic penguins (*Spheniscus magellanicus*) and South American sea lions (*Otaria flavescens*) [41–42]. The 67,197-ha park is also important for other marine mammals such as Antarctic Minke whales (*Balaenoptera bonaerensis*), Orcas (*Orcinus orca*), and southern elephant seals (*Mirounga leonina*).

The waters of the Straits of Magellan are fresher, and cooler than the open shelf waters owing to the effects of melting water from numerous glaciers [43]. The eastward influence of the Pacific by the Antarctic Circumpolar Current (West Wind Drift) reaches Carlos III Island, where a narrow constriction and shallow sill exists, thus constraining water exchange between the Pacific and the Straits [40]. This semi-closed fjord system possesses an extensive and complex seascape that harbors a unique and diverse suite of species [44–45].

Cape Horn is the southernmost headland of the Tierra del Fuego Archipelago, marking the northern boundary of the Drake Passage where three great oceans meet [46]. After European contact in 1616, Cape Horn became a major shipping route for much of the world's commerce prior to the construction of the Panama Canal [47–49]. The weather around Cape Horn is extreme, owing to intense winds, large waves, strong currents, and icebergs, making it notorious as one of the most hazardous shipping route in the world [50].

Cabo de Hornos National Park encompasses the entire Cape Horn Archipelago and is comprised of a series of islands and islets, including the main landmasses of Wollaston and Hermite islands. It was designated a UNESCO Biosphere Reserve in 2005, and is the world's southernmost national park [40]. The terrain is almost entirely treeless peat except for some small wooded areas of beech forest (*Nothofagus* spp., [51]). It is one of the world's hotspot for mosses, liverworts, and lichens, which are resistant to the low temperatures and harsh weather [40,52].

The Diego Ramírez Islands are a small archipelago located on the southern edge of the continental shelf ca. 105 km west-southwest of Cape Horn and ca. 700 km northwest of the South Shetland Islands and the Antarctic Peninsula. The archipelago is divided into a smaller northern group with six islets, and a larger southern group, separated by a 3-km wide pass. The two largest islands, Bartolomé and Gonzalo, both lie in the southern group. Águila Islet, the

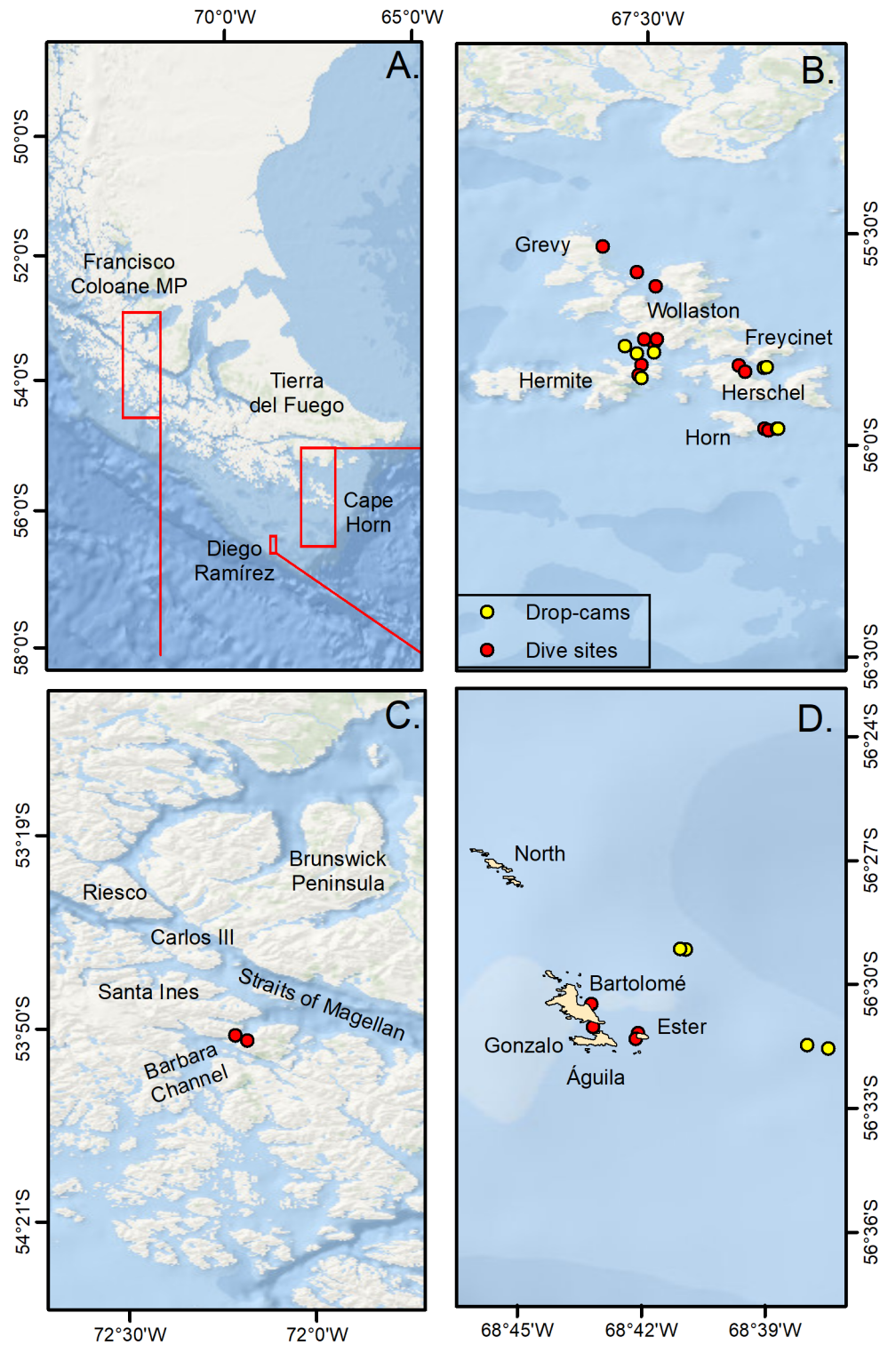


Fig 1. Sampling locations in southern Patagonia. A. Magellan Region, B. Cape Horn Archipelago, C. Francisco Coloane Marine Park, D. Diego Ramirez.

<https://doi.org/10.1371/journal.pone.0189930.g001>

southernmost land of the group, is at 56°32'9"S. These islands are the southernmost inhabited outpost of South America, and are an important nesting site for numerous seabird species, including the black-browed albatross (*Thalassarche melanophris*), grey-headed albatross (*T. chrysostoma*), shy albatross (*Diomedea cauta*), Southern Rockhopper penguin (*Euduptes chrysocome chrysocome*) and Macaroni penguin (*E. chrysolophus*) [53–54].

Benthic surveys

Characterization of the benthos was conducted by scuba divers along two 25-m long transects at each sampling location. Transects were run parallel to the shoreline, with a target depth of 10 m, depending on location of the kelp forest. For sessile and mobile invertebrates, the number of individuals was estimated on 1-m of either side of the transect line (50 m²). For colonial organisms (sponges, some cnidarians, bryozoans, and some tunicates) colonies, rather than individuals, were counted. When a species was extremely abundant (i.e. > 500) along the transect, abundance was estimated considering the number of individuals/colonies m⁻² and scaled to the total area of the transect (50 m²). Only non-cryptic invertebrates ≥1 cm were enumerated. A second diver counted the number of kelp (*Macrocystis pyrifera* and *Lessonia* spp.) stipes within 1-m on either side of the transect. Salinity and temperature measures were recorded using a YSI model 556 handheld multiparameter instrument at Francisco Coloane and a RBR concerto multi-channel logger at Cape Horn and Diego Ramírez.

Giant kelp canopy biomass

Floating canopy of giant kelp was observed over regional scales using the Landsat 8 Operational Land Imager (OLI) multispectral sensor, which provides 30-m spatial resolution imagery over 7 spectral bands in the visible/near-infrared region of the electromagnetic spectrum. Atmospherically-corrected imagery were obtained from the United States Geological Survey (earthexplorer.usgs.gov). Emergent canopy biomass density was estimated from the three sub-regions using Multiple Endmember Spectral Mixing Analysis [55]. This procedure models each pixel as a linear combination of one static kelp canopy endmember and one of 30 seawater endmembers unique to each image. The use of dynamic seawater endmembers accounts for changing water conditions (e.g. phytoplankton blooms, suspended sediments, sunglint) between image dates. The fraction of kelp canopy within each pixel is determined from the model with the lowest root mean squared error. Canopy biomass density was estimated from the derived kelp fraction using an empirical relationship established for giant kelp from diver-based canopy biomass estimates [56]. Regional giant kelp canopy biomass dynamics can be subject to strong seasonal patterns, especially in areas with periodic wave disturbance, nutrient inputs, and increased seasonal light cycles [57–59]. For this reason, only austral summertime imagery was used in the analysis (December 2016 –March 2017) to coincide with anticipated kelp canopy biomass maximums and diver sampling. Areas with persistent cloud cover during this time frame (such as Hermite Island in western Cape Horn) were filled with earlier Landsat 8 imagery for use in figures but were not included in the analysis.

Fish surveys and collections

At each survey site, a scuba diver counted and sized all fishes within 1-m of either side of a 25 m transect line (50 m²). The transect extended to the surface or as far as visibility allowed, including species associated with the kelp canopy and water column. Total fish lengths were estimated to the nearest cm.

Fish collections were conducted opportunistically using several methods. Beach seines (10 x 2 m with 10 mm stretch mesh) were used at Horn and Herschel at Cape Horn and Gonzalo

Island at Diego Ramírez. High-density polyethylene traps (87 × 69 × 29 cm) with 4.5 × 1.8 cm openings (<http://www.fathomsplus.com>) were deployed between 85 and 110 m and baited with ~ 0.5 kg of frozen *Cilus gilberti*. At Diego Ramírez, 3 traps were deployed at each of 2 sites, for 3 hours each, while at Cape Horn, 3 traps were deployed at each of 3 sites, for 3 hours each. Fish were also collected by hand or dip net from beneath stones in the upper to mid-intertidal zone (exposed at low tide).

Deep Ocean Dropcam surveys

National Geographic's Deep Ocean Dropcams are high definition cameras (Sony Handycam HDR-XR520V 12 megapixel) encased in a 43-cm diameter borosilicate glass sphere that are rated to 10,000 m depth. We also deployed a Dropcam Mini, encased in a 33-cm diameter borosilicate glass sphere and rated to 5,000 m. This Dropcam Mini housed a Sony Handycam FDR-AX33 4K Ultra-High Definition video with a 20.6 megapixel still image capability. Viewing area per frame for both cameras was between 2–6 m², depending on the steepness of the slope where the Dropcam landed. Cameras were baited with ~ 1 kg of frozen fish and deployed for 6 to 9 hrs.

The relative abundance of each species was calculated as the maximum number of individuals per frame (MaxN). The substrata for each Dropcam deployment was classified into standard geological categories following Tissot et al. [60]: mud (M), sand (S), pebble (P), cobble (C), boulder (B), continuous flat rock (F), diagonal rock ridge (R), and vertical rock-pinnacle top (T). Seafloor type was defined by a two-letter code representing the approximate percent cover of the two most prevalent substrata in a habitat patch. The first character represented the substratum that accounted for at least 50% of the patch, and the second represented the second most prevalent substratum accounting for at least 30% of the patch.

Statistical analyses

Comparisons of kelp canopy biomass density based on Landsat 8 OLI data among sub-regions (Francisco Coloane, Cape Horn, and Diego Ramírez) was conducted using using a generalized linear model with poisson distribution and log link function. *Post hoc* comparisons between sub-regions were tested using contrasts of the least squares means. *In-situ* measures of kelp taxa densities, and benthic assemblage characteristics (e.g., species richness, numerical abundance, diversity, and evenness) among sub-regions were conducted using a Kruskal-Wallis rank-sum test (X^2), with a Steel-Dwass test for unplanned multiple comparisons in the case of a significant main effect [61]. Benthic taxa diversity was calculated from the Shannon-Weaver diversity index [62]: $H' = -\sum p_i \ln(p_i)$, where p_i is the proportion of all individuals counted that were of taxa i . The evenness component of diversity was expressed as: $J = H' / \ln(S)$, where S is the total number of species present [63]. Benthic taxa were categorized by functional groups based on published literature and were as follows: passive suspension feeder, active suspension feeder, herbivorous/browser, carnivorous, omnivorous, and deposit feeder [64]. Correlations between pooled sea urchin densities and densities of the two kelp genera (*Macrocystis* and *Lessonia*) were compared using Spearman's rank-order correlation (ρ).

Drivers of benthic and fish assemblage structure were investigated using permutation-based multivariate analysis of variance (PERMANOVA, [65]). A Bray–Curtis similarity matrix was created from abundance of benthic taxa, benthic functional groups, and fish species. Sub-region was treated as a fixed factor. Prior to analysis, benthic taxa and functional group abundance data were $\ln(x+1)$ transformed, and fish species abundance was 4th-root-transformed. Interpretation of PERMANOVA results was aided using individual analysis of similarities (ANOSIM), and similarity percentages analysis (SIMPER). The ANOSIM R statistic represents

pairs of sub-regions that are either well separated ($R > 0.75$), overlapping but clearly different ($R > 0.5$), or barely separable at all ($R < 0.25$). SIMPER identified the taxa most responsible for the percentage dissimilarities between islands using Bray-Curtis similarity analysis of hierarchical agglomerative group average clustering [66]. Principal Coordinate Analysis (PCO) was used to compare benthic and fish assemblage structure among sub-regions. All PERMANOVA, PCOs, and SIMPER analyses were conducted using Primer v6 [65].

Results

We conducted a total of 35 transects at 18 locations within the Magellan Region (Francisco Coloane MP = 4, Cape Horn = 23, Diego Ramírez = 8). Transect depths averaged 11.2 ± 2.5 m (range: 7–15 m). During the expedition, water temperatures at 10 m around Francisco Coloane MP averaged $8.8^\circ\text{C} (\pm 0.2)$, while temperatures were nearly a degree higher at Cape Horn ($\bar{X} = 9.7^\circ\text{C} \pm 0.2$) and Diego Ramírez ($\bar{X} = 9.7^\circ\text{C} \pm 0.1$). Salinity averaged $30.1\text{‰} (\pm 0.1)$ at Francisco Coloane, $33.1\text{‰} (\pm 0.2)$ at Cape Horn, and $33.5\text{‰} (\pm 0.1)$ at Diego Ramírez.

Benthic communities

Kelp forests were the dominant nearshore marine ecosystem in the Magellan Region, with the giant kelp *Macrocystis pyrifera* being the most conspicuous component of this community. In many locations, the large brown seaweed *Lessonia* spp. formed dense understories within the *Macrocystis* canopy. Based on Landsat 8 OLI data, kelp canopy biomass was most dense at the Cape Horn Archipelago with a mean canopy biomass density of $2.51 \text{ kg m}^{-2} (\pm 1.27 \text{ sd})$, followed by Diego Ramírez with $2.29 \text{ kg m}^{-2} (\pm 0.78 \text{ sd})$, and Francisco Coloane with $2.14 \text{ kg m}^{-2} (\pm 1.07 \text{ sd})$. Canopy biomass density was significantly higher at Cape Horn compared to Diego Ramírez, with was in turn significantly higher than Francisco Coloane ($X^2 = 44.7, p < 0.001$; $\text{CH} > \text{DR} > \text{FC}$). Kelp extent was higher on the eastern and northern coasts of the Cape Horn Archipelago, likely due to shelter from the prevailing wind and swell that originate from the west (Fig 2).

Overall *in situ* densities of *M. pyrifera* ($\bar{X} = 4.65 \pm 2.86 \text{ no. m}^{-2}$) were nearly three times higher than densities of *Lessonia* spp. ($\bar{X} = 1.62 \pm 1.78, X^2 = 24.1, p < 0.001$). Stipe densities of *M. pyrifera* were not significantly different among sub-regions ($X^2 = 4.9, p = 0.08$), although densities at Diego Ramírez were 77% higher than at Francisco Coloane and 50% higher than at Cape Horn (Fig 3). Densities of *Lessonia* spp. were significantly higher at Diego Ramírez compared with Cape Horn and Francisco Coloane ($X^2 = 13.3, p = 0.001$), which were statistically indistinguishable despite 2-fold high densities at Cape Horn compared to Francisco Coloane.

We recorded 122 invertebrate taxa from 18 classes or infraclasses and 10 phyla during our surveys (S1 Table). Mollusks were the richest phyla with 32 taxa, followed by echinoderms with 20, and sponges with 18. Of the mollusks, gastropods were by far the most specious and abundant. The average number of benthic taxa per transect was highest in the Cape Horn Archipelago and nearly 50% lower at Francisco Coloane (Table 1). The order of magnitude greater abundance of individuals at Cape Horn was driven by the bivalve *Gaimardia trapesina*. If this species is excluded, average numerical density was still significantly greater at Cape Horn ($\bar{X} = 13.0 \pm 9.5$) compared with Diego Ramírez ($p = 0.02$), but not Francisco Coloane ($p = 0.31$). Diversity and evenness were both highest at Diego Ramírez and lowest in Francisco Coloane MP.

There was a significant difference in the assemblages of benthic taxa among sub-regions (PERMANOVA Pseudo- $F_{2,34} = 7.64, p < 0.001$). Benthic assemblages based on taxa abundance at Francisco Coloane were distinct from Diego Ramírez (ANOSIM $R = 0.987$) and Cape Horn ($R = 0.898$). Although also significant ($p < 0.001$), the benthic assemblages between Cape

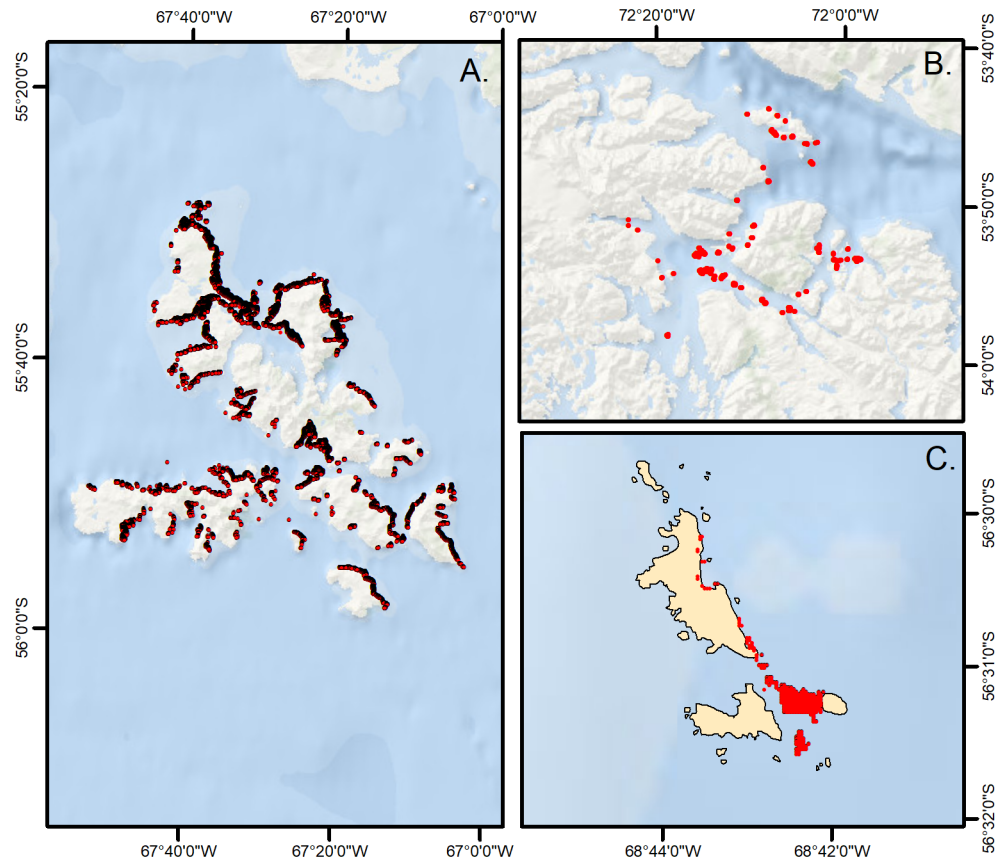


Fig 2. Kelp areal coverage derived from Landsat 8 satellite Operational Land Imager multispectral sensor. A.—Cape Horn, B. Francisco Coloane Marine Park, C. Diego Ramírez.

<https://doi.org/10.1371/journal.pone.0189930.g002>

Horn and Diego Ramírez were more similar to one another compared to the other pair-wise comparisons ($R = 0.634$).

There was clear separation of sampling locations by sub-region in ordination space and relatively high concordance within sub-regions based on taxa abundance (Fig 4). PCO1 explained nearly 23% of the variation in benthic taxa distribution among the three sub-regions, with the strongest separation between Diego Ramírez and the other two sub-regions. PCO2 explained an additional 16% of the variation and separated Cape Horn from Francisco Coloane. The sea star *Porania antarctica* drove the separation of Francisco Coloane, while the sea star *Cosmasterias lurida* and the painted shrimp *Campylonotus vagans* drove the separation of sites around Cape Horn. The encrusting red sponge *Scopalina* sp., the colonial tunicate *Aplidium* sp., the colonial arborescent bryozoan *Bugula* sp., and the encrusting bryozoan *Beania magellanica* accounted for the separation of Diego Ramírez.

The sea cucumber *Cladodactyla crocea croceoides* accounted for 73.1% of the total numerical abundance at Francisco Coloane, followed by the colonial tunicate *Didemnum studeri* (7.3%), the barnacle *Notobalanus flosculus* (6.7%), and the sea urchin *Arbacia dufresnii* (4.6%) (Table 2). The bivalve *Gaimardia trapesina* comprised 74.2% of benthic taxa abundance at Cape Horn, followed by the barnacle *Balanus* cf. *laevis* (4.0%), the false king crab *Paralomis granulosa* (2.7%), and the carnivorous top snail *Argobuccinum ranelliforme* (2.4%). Diego Ramírez showed greater diversity among taxa, with the bryozoan *Bugula* sp. (13.9%), the sea

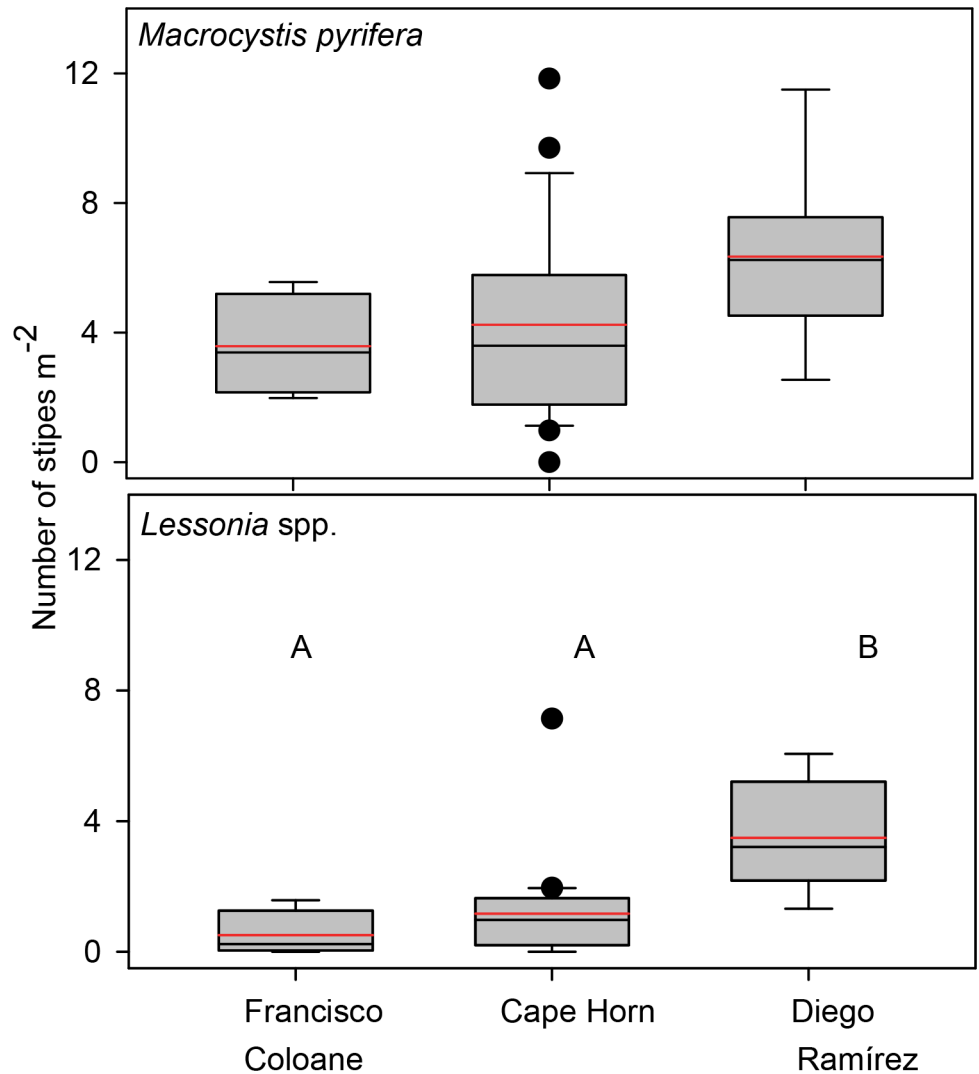


Fig 3. Stipe densities of *Macrocytis pyrifera* and *Lessonia* spp. among the three sub-regions. Box plots showing median (black line), mean (red dashed line), upper and lower quartiles, and 5th and 95th percentiles. Kruskal-Wallis Rank Sum comparisons among regions were statistically different for *Lessonia* spp. ($X^2 = 13.3$, $p = 0.001$) but not for *Macrocytis pyrifera* ($X^2 = 4.9$, $p = 0.08$). Regions with the same letter are not significantly different (Steel-Dwass unplanned multiple comparisons procedures, $\alpha = 0.05$).

<https://doi.org/10.1371/journal.pone.0189930.g003>

Table 1. Benthic assemblage characteristics among sub-regions. Diversity is Shannon-Wiener $H'(\log_e)$, Evenness is $J = H'/\ln(S)$. Statistical results of Kruskal-Wallis rank-sum test (X^2) with Steel-Dwass test for unplanned multiple comparisons. Underlined sub-regions are not significantly different ($\alpha = 0.05$). Francisco Coloane = FC, Cape Horn = CH, Diego Ramírez = DR.

Metric	Francisco Coloane	Cape Horn	Diego Ramírez	X^2	P	Multiple comparisons
Species (S)	15.00 (5.48)	29.87 (7.61)	25.50 (3.63)	11.08	0.004	<u>CH</u> <u>DR</u> FC
No. m^{-2}	7.13 (10.32)	50.22 (82.63)	5.47 (1.05)	9.45	0.009	CH <u>FC</u> <u>DR</u>
Diversity	1.37 (0.67)	1.95 (0.80)	2.50 (0.22)	6.51	0.039	<u>DR</u> CH FC
Evenness	0.51 (0.25)	0.59 (0.23)	0.77 (0.04)	8.34	0.015	DR <u>CH</u> <u>FC</u>

<https://doi.org/10.1371/journal.pone.0189930.t001>

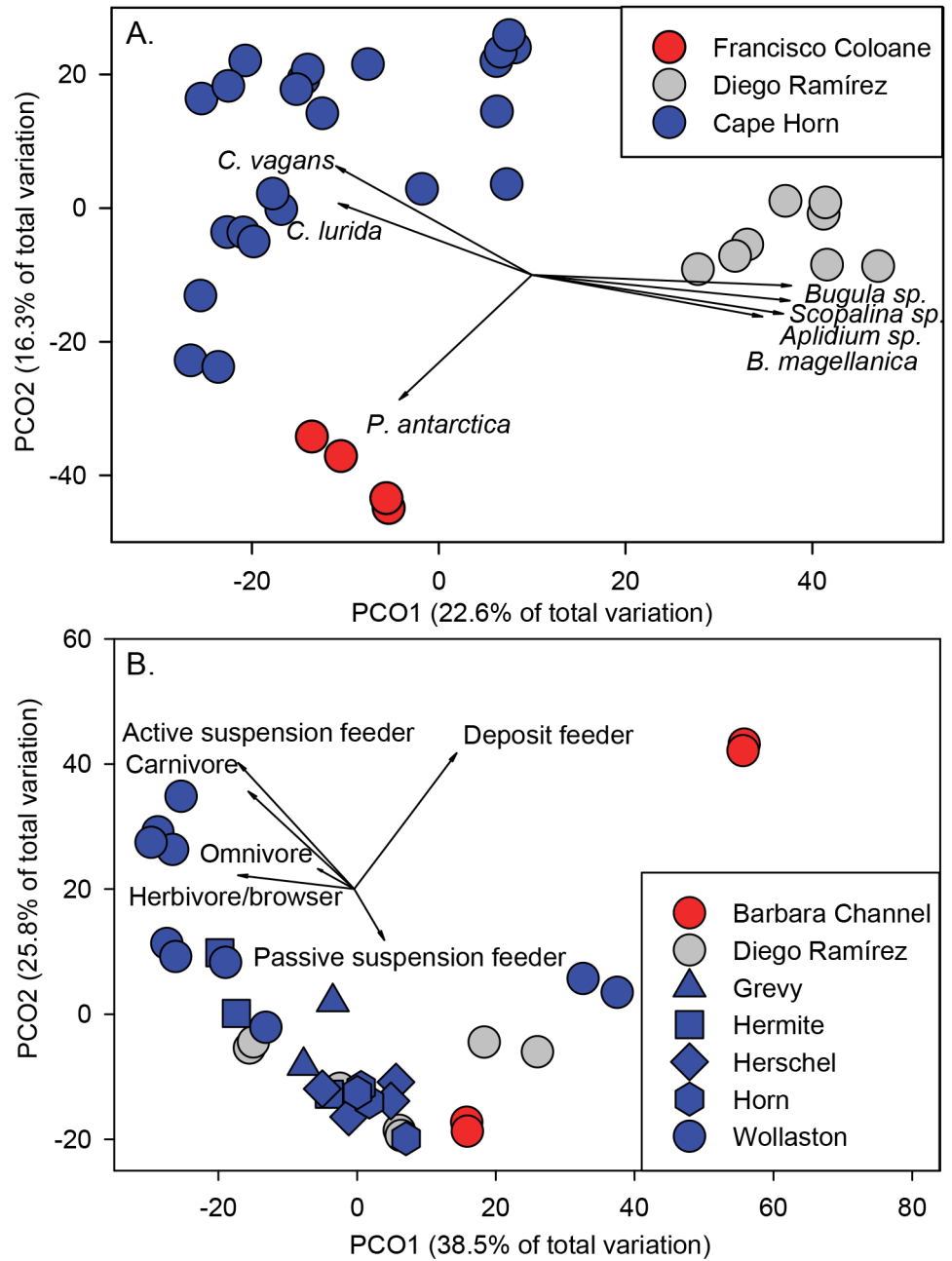


Fig 4. Principle coordinates analysis of A. benthic taxa by sub-region and, B. functional groups by island within sub-regions. Benthic taxa and functional group abundance data were $\ln(x+1)$ transformed prior to analyses. Vectors are the primary taxa driving the ordination (Pearson Product movement correlations ≥ 0.6). *C. vagans*–*Campylonotus vagans*, *C. lurida*–*Cosmasterias lurida*, *P. antarctica*–*Porania antarctica*.

<https://doi.org/10.1371/journal.pone.0189930.g004>

urchin *Loxechinus albus* (12.3%), the sea snail *Tegula atra* (11.3%) being the most abundant benthic taxa around Diego Ramírez.

The dissimilarity in benthic assemblages based on taxa abundance between Francisco Coloane and Cape Horn was 95.0% and was driven by the abundance of *G. trapesina* at Cape Horn and *C. crocea croceoides* in the fjords. The dissimilarity between Francisco Coloane and Diego Ramírez was also high (95.5%), with *Bugula sp.*, *L. albus*, and *T. atra* at Diego Ramírez

Table 2. Similarity of percentages (SIMPER) for benthic taxa most responsible for the percent dissimilarities between sub-regions using Bray-Curtis similarity analysis of hierarchical agglomerative group average clustering. Values are mean (no. m⁻²) with standard deviations in parentheses. Diss. = Average dissimilarity with one standard deviation of the mean in parentheses. A = Cape Horn and Diego Ramírez, B = Cape Horn and Francisco Coloane, and C = Diego Ramírez and Francisco Coloane.

A	Cape Horn	Diego Ramírez	Diss.	% Diss.
Dissimilarity = 90.50				
<i>Gaimardia trapesina</i>	37.24 (76.68)	0.01 (0.02)	21.0 (0.6)	23.2
<i>Balanus cf. laevis</i>	1.98 (3.26)	-	6.2 (0.5)	6.8
<i>Loxechinus albus</i>	0.6 (1.31)	0.67 (0.26)	4.5 (1.3)	5.0
<i>Bugula sp.</i>	0.05 (0.12)	0.76 (0.83)	4.1 (0.7)	4.5
<i>Didemnum studeri</i>	0.79 (1.99)	0.22 (0.35)	4.1 (0.4)	4.5
<i>Tegula atra</i>	0.34 (1.12)	0.62 (0.61)	4.0 (0.9)	4.4
<i>Pagurus comptus</i>	0.73 (1.43)	-	3.3 (0.6)	3.7
B	Cape Horn	Francisco Coloane	Diss.	% Diss.
Dissimilarity = 95.02				
<i>Gaimardia trapesina</i>	37.24 (76.68)	-	21.0 (0.6)	22.0
<i>Cladodactyla crocea croceoides</i>	-	5.21 (9.87)	14.2 (0.6)	14.9
<i>Balanus cf. laevis</i>	1.98 (3.26)	-	6.5 (0.5)	6.8
<i>Didemnum studeri</i>	0.79 (1.99)	0.52 (0.99)	4.9 (0.5)	5.2
<i>Pagurus comptus</i>	0.73 (1.43)	-	3.6 (0.6)	3.8
C	Diego Ramírez	Francisco Coloane	Diss.	% Diss.
Dissimilarity = 95.47				
<i>Cladodactyla crocea croceoides</i>	-	5.21 (9.87)	21.0 (0.7)	21.2
<i>Bugula sp.</i>	0.76 (0.83)	-	8.2 (0.9)	8.6
<i>Loxechinus albus</i>	0.67 (0.26)	-	7.7 (1.7)	8.0
<i>Tegula atra</i>	0.62 (0.61)	-	6.9 (0.9)	7.2
<i>Notobalanus flosculus</i>	-	0.48 (0.95)	5.2 (0.6)	5.4
<i>Scopalina sp.</i>	0.42 (0.38)	-	5.2 (0.9)	5.4
<i>Ophiactis asperula</i>	-	0.33 (0.43)	5.2 (0.9)	5.2

<https://doi.org/10.1371/journal.pone.0189930.t002>

and *C. crocea croceoides* in the fjords driving the difference. The dissimilarity between Cape Horn and Diego Ramírez was 90.5% with *G. trapesina* and *B. laevis* at Cape Horn and *Bugula sp.*, and *L. albus* at Diego Ramírez accounting for the differences.

Benthic functional groups among regions

Active suspension feeders comprised 79.5% of overall numerical abundance within the benthic assemblages, of which *G. trapesina* accounted for 87.8% of this total. If this species is excluded, then active suspension feeders accounted for 32.1% of functional group abundance, followed by carnivores (31.7%), herbivores/browsers (22.2%), and passive suspension feeders (10.5%).

There was a significant difference in the assemblages of benthic functional groups among sub-regions (Pseudo-F_{2,34} = 6.37, p < 0.001). Benthic assemblages based on taxa at Francisco Coloane were distinct from Diego Ramírez (ANOSIM R = 0.741) and Cape Horn (R = 0.711), but indistinguishable between Cape Horn and Diego Ramírez (R = 0.091). Benthic assemblage structure based on abundance by functional group showed less separation among sub-regions, but identified a few unique locations that stood out from the rest (Fig 4). The two transects at Station 1 located in Canal Barbara within Francisco Coloane MP were extreme outliers from all other stations and were explained by the high abundance of the deposit feeding ophiuroid, *Ophiactis asperula*. Despite deposit feeders comprising only 1.1% of overall functional group abundance, this species accounted for 59.1% of the abundance at this location. Active suspension feeders (primarily *G. trapesina* and *Balanus sp.*), carnivores (primarily the sea star

Table 3. Sea urchin numerical abundances among sub-regions. Values are mean (no. m⁻²) with standard deviations in parentheses.

Sea urchin species	Francisco Coloane	Cape Horn	Diego Ramírez	Percentage of total
<i>Loxechinus albus</i>	-	0.60 (1.31)	0.67 (0.26)	59.1
<i>Arbacia dufresnii</i>	0.06 (0.06)	0.22 (0.43)	0.17 (0.18)	20.9
<i>Pseudechinus magellanicus</i>	0.03 (0.04)	0.35 (0.43)	0.01 (0.02)	18.1
<i>Austrocidaris canaliculatum</i>	0.01 (0.01)	0.02 (0.04)	0.01 (0.01)	1.4
Percentage of total	4.7	55.6	39.7	

<https://doi.org/10.1371/journal.pone.0189930.t003>

C. lurida), and the predatory sea snail *Argobuccinum ranelliforme* were most responsible for separating Stations 13 and 14 at Wollaston Island, within the Cape Horn Archipelago, from most other locations.

Sea urchins are important components of the herbivore/browser functional assemblage. Overall densities of sea urchins were highest at Cape Horn followed by Diego Ramírez, with Francisco Coloane having 9 to 12 times lower densities, respectively, compared to the other locations (Table 3). *Loxechinus albus* accounted for 59% of all sea urchins, with similar densities between Cape Horn and Diego Ramírez, but they were completely absent from Francisco Coloane. *Arbacia dufresnii* and *Pseudechinus magellanicus* comprised an additional 21% and 18%, respectively, of overall sea urchin abundance. There were no significant correlations between the total density of all sea urchins combined and densities of either *Lessonia* ($\rho = 0.20$, $p = 0.26$) or *Macrocystis* ($\rho = 0.23$, $p = 0.18$). The sea star *C. lurida* is a predator on sea urchins and densities of this species was an order of magnitude higher at Cape Horn ($\bar{X} = 0.43 \pm 0.42$), compared with both Francisco Coloane ($\bar{X} = 0.04 \pm 0.03$) and Diego Ramírez ($\bar{X} = 0.02 \pm 0.02$, $X^2 = 16.6$, $p = 0.003$, CH > FC = DR).

Fishes

A total of 18 species of fishes from 12 families were observed during shallow water (<40 m) surveys (Table 4). Of these, 14 were observed on quantitative transects, with the average size of all species combined only 9.7 cm TL (± 4.9). The blennioid *Calliclinus geniguttatus* ($n = 2$, $\bar{X} = 26.5 \pm 4.9$ cm TL) and the southern hagfish *Myxine australis* ($n = 3$, $\bar{X} = 21.7 \pm 7.6$ cm TL) were the only two species larger than 20 cm TL observed on transects.

Collections in the rocky intertidal yielded four species, two cod icefishes (*Patagonotothen cornucola*, *P. sima*), the Magellan plunderfish (*Harpagifer bispinis*) and an eelpout (*Austrolycus depressiceps*), with the latter two species only observed in the rocky intertidal zone. Beach seining yielded one Patagonian blenny or rockcod (*Eleginops maclovinus*, 26 cm TL) at Herschel Island, 40 Fuegian sprat (*Sprattus fuegensis*, $\bar{X} = 7$ cm TL) at Horn Island, and the Magellanic rockcod (*P. magellanica*), which were caught at Horn Island ($n = 1$, 5.0 cm TL), and Gonzalo Island ($n = 5$, $\bar{X} = 7.5 \pm 1.8$ cm TL).

Traps resulted in the capture of one narrowmouthed catshark (*Schroederichthys biviuis*, 35 cm TL), one Magellanic ray (*Bathyraja magellanica*, ~ 25 cm disk width), two cod icefish (*P. cornucola*, 12 and 14 cm TL), and 24 southern hagfish (range 30–50 cm TL). Trap catch rates were similarly low between Diego Ramírez (0.66 [± 0.63 sd] fish per trap hour, $n = 18$ total trap hrs) and Cape Horn (0.59 [± 0.43 sd] fish per trap hour, $n = 27$ total trap hrs).

The number of fish species observed on transects was significantly higher ($X^2 = 7.1$, $p = 0.03$) at Diego Ramírez ($\bar{X} = 3.3 \pm 1.06$) compared with Cape Horn ($\bar{X} = 2.3 \pm 0.7$) and Francisco Coloane ($\bar{X} = 2.3 \pm 1.0$), which were not significantly different from one another. The number of individual fishes was nearly 10 times higher at Diego Ramírez

Table 4. Shallow water fish species observed during surveys in the Magellan Region. Mean total length (TL) in cm are from quantitative underwater transects unless otherwise noted.

Order	Family	Species	Mean TL (sd)
Myxiniiformes	Myxiniidae	<i>Myxine australis</i>	21.7 (7.6)
Carcharhiniiformes	Scyliorhinidae	<i>Schroederichthys biviuis</i> ⁺	35.0
Rajiformes	Arhynchobatidae	<i>Bathyraja magellanica</i> ⁺	25.0
Clupeiformes	Clupeidae	<i>Sprattus fuegensis</i> [#]	7.0 (1.0)
Scorpaeniformes	Sebastidae	<i>Sebastes oculatus</i>	24.0
	Agonidae	<i>Agonopsis chilensis</i>	9.0 (1.4)
Perciformes	Zoarcidae	<i>Austrolycus depressiceps</i> [*]	15.0 (10.0)
		<i>Piedrabuenia ringueleti</i>	12.0
	Bovichtidae	<i>Cottoperca trigloides</i>	11.0 (7.6)
	Nototheniidae	<i>Paranotothenia magellanica</i>	10.6 (3.2)
		<i>Patagonotothen brevicauda</i>	10.5 (1.2)
		<i>Patagonotothen cornucola</i>	10.8 (3.4)
		<i>Patagonotothen sima</i>	6.0 (1.8)
		<i>Patagonotothen squamiceps</i>	7.4 (2.3)
		<i>Patagonotothen tessellata</i>	8.7 (3.1)
	Eleginopsidae	<i>Eleginops maclovinus</i> [#]	26.0
	Harpagiferidae	<i>Harpagifer bispinis</i> [*]	4.5 (0.8)
Labrisomidae	<i>Calliclinus geniguttatus</i>	26.5 (4.9)	

*Intertidal hand collection only,

+Trap only,

#Beach seine only.

<https://doi.org/10.1371/journal.pone.0189930.t004>

($\bar{X} = 0.70 \pm 0.38$) compared with Francisco Coloane ($\bar{X} = 0.07 \pm 0.04$), and four times higher at Cape Horn ($\bar{X} = 0.57 \pm 0.63$) compared with Francisco Coloane (Fig 5).

There were clear differences in the fish assemblages between Diego Ramírez and the other two sub-regions, with PCO1 explaining 62.5% of the total variation (Fig 6). These differences were driven by the cod icefishes *P. sima* and *P. brevicauda* at Diego Ramírez. The two stations at Horn Island, at the extreme southern tip of the Cape Horn Archipelago, were most similar to the fish assemblage at Diego Ramírez, likely due to similar exposed oceanic environments. Another cod icefish, *P. cornucola*, was most common in the fjords and protected locations within the Cape Horn Archipelago.

There was 100% dissimilarity in the fish assemblages between Francisco Coloane and Diego Ramírez, which was primarily driven by the high density of *P. sima* at Diego Ramírez (Table 5). Similarly, there was a 93% dissimilarity in the fish assemblages between Cape Horn and Diego Ramírez, driven by the high density of *P. sima* at Diego Ramírez and *P. tessellata* at Cape Horn (Fig 6). Dissimilarity between Cape Horn and the fjords was 79% with low densities of all species in the fjords.

Mesophotic habitats

We conducted 12 Deep Ocean Dropcam deployments ranging in depth from 53 to 105 m ($\bar{X} = 79 \pm \text{SD } 16.5$), with recording times ranging from 89 to 364 min ($\bar{X} = 231 \pm \text{SD } 98$, Table 6). The most common habitat encountered was sand and cobble, followed by mud and pebbles. Unique habitats included a diagonal rock ridge at 100 m, and a boulder field at 87 m.

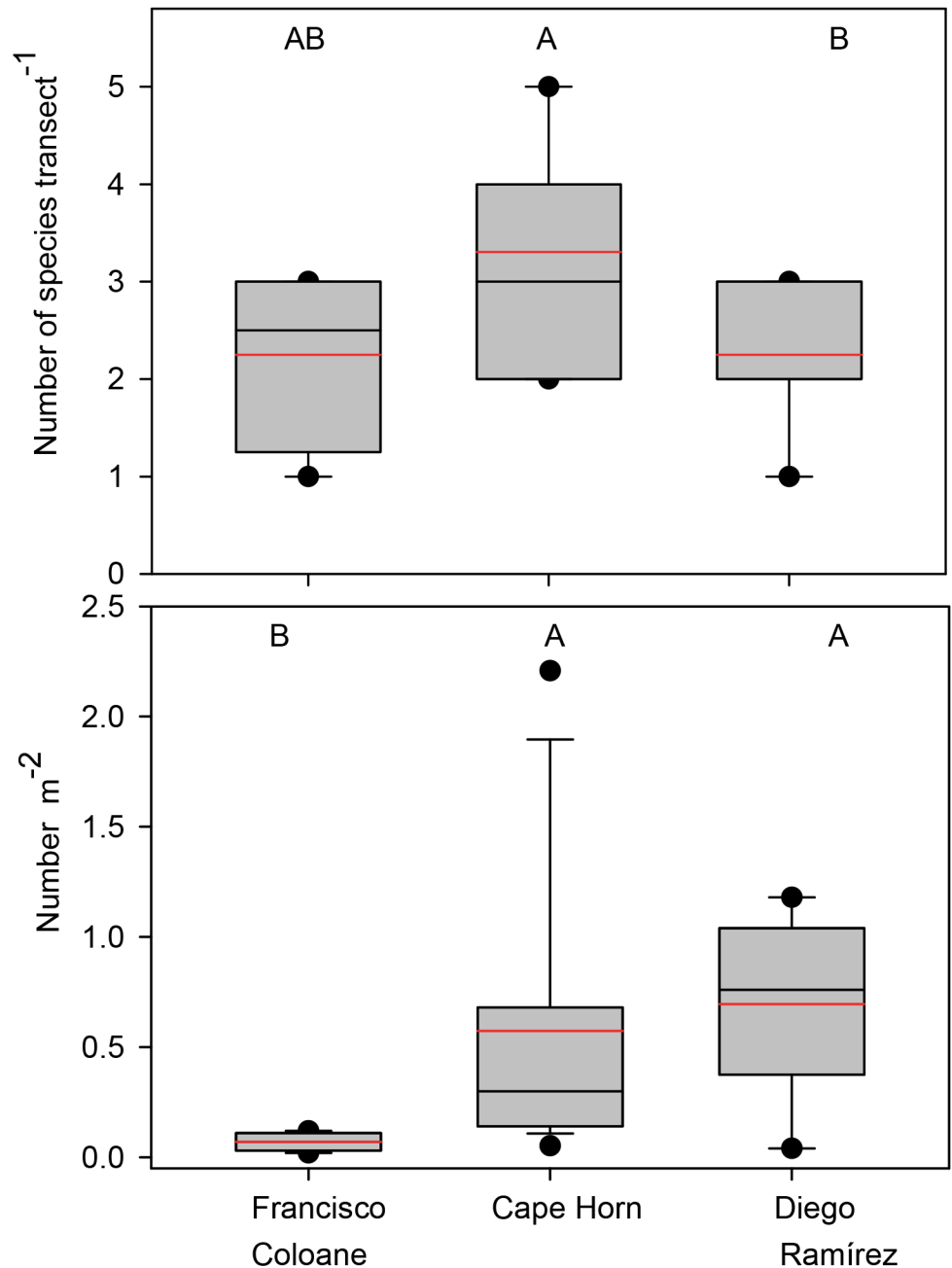


Fig 5. Fish assemblage characteristics among the three sub-regions. Box plots showing median (black line), mean (red dashed line), upper and lower quartiles, and 5th and 95th percentiles. Kruskal-Wallis Rank Sum comparisons among regions were statistically different for species richness ($X^2 = 13.3$, $p = 0.001$) and numerical abundance ($X^2 = 4.9$, $p = 0.08$). Regions with the same letter are not significantly different (Steel-Dwass unplanned multiple comparisons procedures, $\alpha = 0.05$).

<https://doi.org/10.1371/journal.pone.0189930.g005>

Thirty taxa from 25 families, 15 classes, and 7 phyla were observed on our Deep Ocean Dropcam deployments (S2 Table). Sponges were observed on 75% of the deployments and covered as much as 30% of the benthos on one occasion at 95 m on pebble and cobble habitat. Bryozoans were common between 87 and 105 m, and covered up to 20% of the substrate on sand and cobble habitat. Five taxa of cnidarians were observed from four different orders,

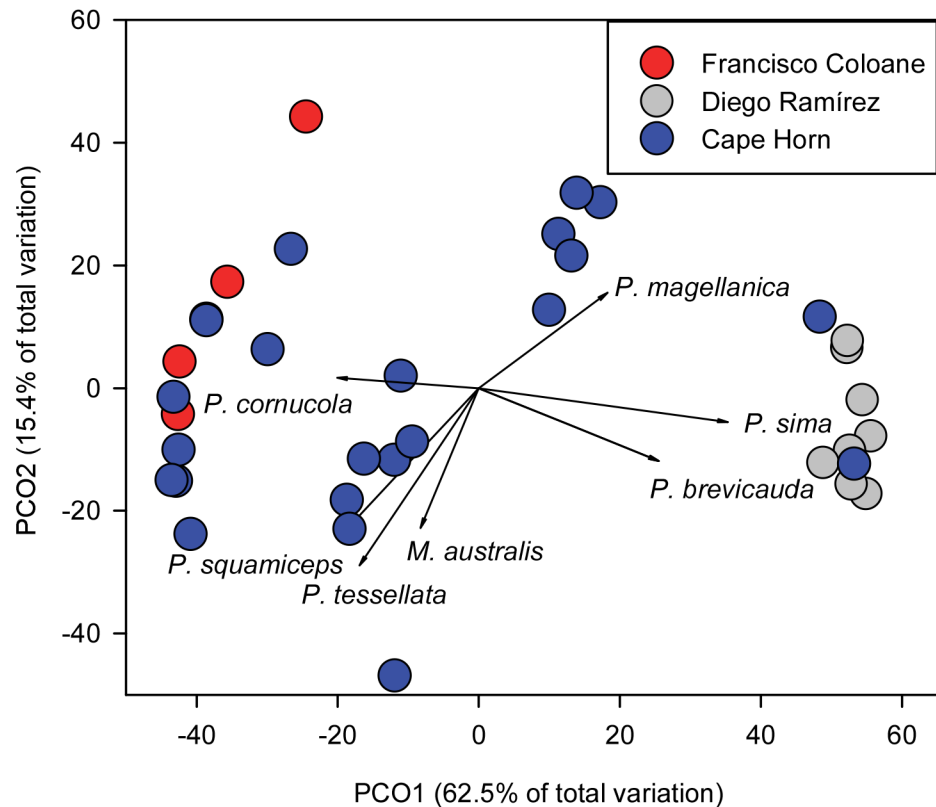


Fig 6. Principle coordinates analysis of fish species numerical abundance by sub-region. Data were 4th root transformed prior to analyses. Vectors are the primary taxa driving the ordination (Pearson Product movement correlations ≥ 0.3). P. spp.—*Patagonotothen* spp. except for *P. magellanica*—*Paranotothenia magellanica*. *M. australis*—*Myxine australis*, *C. geniguttatus*—*Calliclinus geniguttatus*.

<https://doi.org/10.1371/journal.pone.0189930.g006>

including hydrocoral (*Errina antarctica*, Stylasteridae), hard coral (*Tethocyathus endesa*, Caryophylliidae), octocoral (Primnoidae), and anemones (*Paranthus niveus*, Actinostolidae). Octocorals and hydrocorals were most frequently observed (17% of deployments), with octocorals the most dominant numerically. The hard coral *T. endesa* was only observed on one deployment (100 m on continuous flat rock habitat), where it covered 5% of the benthos.

Of the mobile invertebrates, echinoderms were relatively diverse, with seven species from seven different orders observed. The sea star *C. lurida* was the most frequently observed, occurring on 25% of the deployments. Another sea star *Cycethra verrucosa* was the most numerically dominant echinoderm, with eight observed at one site on sand and cobble (84 m), averaging 0.7 individuals per deployment. Three different orders of mollusks were observed, including clams (*Nucula pisum*, Nuculidae), octopus (*Robsonella fontaniana*, Octopodidae) and sea snails (*Adelomelon ancilla* and *Odontocymbiola magellanica*, Volutidae).

The southern hagfish was the most frequently encountered of the mesophotic fishes (50% frequency of occurrence), primarily on sand and cobble habitat in depths ranging from 65 to 105 m. The cod icefish (*P. cornucola*) were the next most abundant of these fishes (17% frequency of occurrence), and were found in depths ranging from 85 to 105 m on sand and cobble habitat. The Fuegian sprat was the most abundant fish species by number, averaging 5.7 per site, but was only found at three sites. Their maximum number (MaxN = 29) occurred at 105 m depth in sand and cobble habitat. The Patagonian redfish (*Sebastes oculatus*, Sebastidae) was observed between 84 and 87 m on boulder, sand, and cobble habitat (17% frequency of

Table 5. Similarity of percentages (SIMPER) for fish species most responsible for the percent dissimilarities between sub-regions using Bray-Curtis similarity analysis of hierarchical agglomerative group average clustering. Values are mean (no. m⁻²) with standard deviations in parentheses. Diss. = Average dissimilarity with one standard deviation of the mean in parentheses.

A	Francisco Coloane	Cape Horn	Diss.	% Diss.
Dissimilarity = 79.15				
<i>Patagonotothen tessellata</i>	0.03 (0.03)	0.33 (0.56)	31.3 (1.0)	39.55
<i>Patagonotothen squamiceps</i>	0.01 (0.01)	0.12 (0.17)	20.1 (1.0)	25.37
<i>Patagonotothen sima</i>	-	0.03 (0.03)	9.7 (0.7)	12.22
<i>Patagonotothen cornucola</i>	0.03 (0.01)	0.06 (0.06)	9.4 (1.0)	11.87
<i>Paranotothenia magellanica</i>	-	0.02 (0.05)	6.6 (0.5)	8.38
B	Francisco Coloane	Diego Ramírez	Diss.	% Diss.
Dissimilarity = 100.00				
<i>Patagonotothen sima</i>	-	0.65 (0.37)	76.6 (3.3)	76.57
<i>Patagonotothen cornucola</i>	0.03 (0.01)	-	7.3 (0.8)	7.26
<i>Patagonotothen tessellata</i>	0.03 (0.03)	-	6.1 (0.6)	6.06
<i>Patagonotothen breviceauda</i>	<0.01 (0.01)	0.01 (0.01)	4.0 (0.6)	3.96
C	Cape Horn	Diego Ramírez	Diss.	% Diss.
Dissimilarity = 92.99				
<i>Patagonotothen sima</i>	0.03 (0.03)	0.65 (0.37)	51.5 (2.0)	55.41
<i>Patagonotothen tessellata</i>	0.33 (0.56)	-	17.9 (0.7)	19.21
<i>Patagonotothen squamiceps</i>	0.12 (0.17)	-	10.1 (0.8)	10.82
<i>Patagonotothen cornucola</i>	0.06 (0.06)	-	6.4 (0.9)	6.85

<https://doi.org/10.1371/journal.pone.0189930.t005>

occurrence). Of the cartilaginous fishes (Chondrichthyes), the narrowmouthed catshark, was observed on one occasion at 87 m in boulder and cobble habitat. The Magellan skate (*Bathyr-
aja magellanica*, Arhynchobatidae) was observed on two occasions between 85 m and 87 m on boulder, cobble, and sand habitat.

Discussion

The extensive kelp forests that dominate the Magellan Region play a key role in structuring the entire ecosystem of the area [67]. The high heterogeneity in the benthic communities that we observed are likely due to the extreme environmental conditions and the highly complex

Table 6. Deep Ocean Dropcam deployment statistics and associated habitats. Habitats: mud (M), sand (S), pebble (P), cobble (C), boulder (B), continuous flat rock (F), diagonal rock ridge (R), and vertical rock-pinnacle top (T). The first letter represents at least 50% cover by that category, and the second, at least 30% cover. Combined, the two-letter code represents ≥ 80% of the benthic cover at a site. Deploy–deployment.

Deploy.	Sub-region	Island	Lat.	Long.	Time (min)	Depth (m)	Benthic (50%)	Benthic (30%)
1	Cape Horn	Horn	-55.961	-67.194	100	53	S	S
2	Cape Horn	Horn	-55.962	-67.192	270	60	S	S
3	Diego Ramírez	Gonzalo	-56.486	-68.682	130	87	B	C
4	Diego Ramírez	Gonzalo	-56.486	-68.684	360	95	P	C
5	Diego Ramírez	Bartolomé	-56.524	-68.633	355	85	S	S
6	Diego Ramírez	Bartolomé	-56.526	-68.625	186	84	S	C
7	Cape Horn	Freycinet	-55.817	-67.226	167	105	S	C
8	Cape Horn	Freycinet	-55.816	-67.218	364	100	F	F
9	Cape Horn	Hermite	-55.842	-67.514	254	76	M	M
10	Cape Horn	Hermite	-55.783	-67.525	89	75	S	S
11	Cape Horn	Wollaston	-55.781	-67.485	251	63	S	P
12	Cape Horn	Wollaston	-55.767	-67.554	253	65	S	C

<https://doi.org/10.1371/journal.pone.0189930.t006>

coastline of the region [67]. The southern Patagonian marine community has affinities with the Antarctic region, distinct from the rest of Chile, with the faunal break ($\sim 55^\circ\text{S}$) largely due to the strong currents that sweep through the Straights of Magellan [68]. Although the region is less diverse than in the north of the country, it has high biodiversity value due to relatively high endemism [68]. During the voyage of the Beagle, Darwin noted the lush kelp forests of Tierra del Fuego and the high diversity of species found within them [32]. Despite being the most southern kelp forests in the world, few ecological studies of this important ecosystem have been conducted [39], and prior to our expedition, none had been undertaken at Diego Ramírez. While our sampling effort provided limited inferential power in terms of the long-term drivers of marine biodiversity within the region, it serves as a value baseline for future investigation of this poorly studied region.

Kelp stipe density and overall marine diversity were highest at Diego Ramírez compared with Cape Horn and Francisco Coloane MP, while its regional kelp canopy density was equal to that of Cape Horn but presented less spatial variability. Dayton [16] noted that kelp in wave protected areas of the southern Magellanic fjords appeared brittle and unhealthy due to shading by surface kelp blades. In addition, there is a strong salinity gradient within the region, which ranges from 20 to 25 ppt in the fjords of Francisco Coloane MP, between 30 and 33 ppt within the Cape Horn Archipelago, and 33–34 ppt at Diego Ramírez [69]. The differences in wave exposure and salinity likely account for the differences in kelp densities that we observed. The higher benthic assemblage richness at Cape Horn was likely due to diversity of habitats in the archipelago with numerous protected coves and bays, as well as exposed shorelines.

Many of the kelp forests in the northern hemisphere have been dramatically altered due to the removal of top predators and the associated proliferation of grazing herbivores, with impacts in some areas having occurred centuries ago [2,16–17,70–72]. The herbivore-kelp dynamics in southern Chile differs greatly from those in the northern hemisphere [73–75]. The Magellan Region is described as having dense *Macrocystis* forests with few sea urchins [76–77]. Four sea urchin species (*L. albus*, *P. magellanicus*, *A. dufresnii* and *A. canaliculata*) in the region are known to feed on kelp; however, these species subsist primarily on drift algae and rarely graze directly on *Macrocystis* [39]. The *Macrocystis* beds in central-southern Chile do not appear to be controlled by sea urchins in exposed sites, and the main herbivores are the gastropod *T. atra* in protected sites [78]. We observed *T. atra* in abundance in some sheltered locations during our expedition, particularly around Cape Horn and at Diego Ramírez where they are presumably more exposed.

Kelp forests within this region are dynamic in space and time, and regulated by wave action, interspecific competition, and substratum availability [74,76–77]. Nearshore edges of kelp beds are constrained by interspecific competition with *Lessonia*, while the seaward extent is limited by substrate availability [77]. Dayton [73] also noted that *Macrocystis* distribution and abundance was negatively affected by entanglement with drift algae and heavy settlement by bivalve mollusks on kelp fronds.

In several sheltered locations at Cape Horn, we observed kelp plants being sunk by the weight of dense aggregations of the bivalve *G. trapesina* that completely covered the kelp fronds and were being preyed upon by the sea star *C. lurida*, which is the most conspicuous predator in the kelp forests of the region [75,79]. Similar observations were made in the fjord region in the 1970s by Dayton [73]. This brooding pelecypod is known to have long larval duration and wide dispersal capabilities due to kelp rafting [80], and was numerically abundant around Wollaston Island but absent from our sampling stations in the fjords. Only a few *G. trapesina* individuals were observed at Diego Ramírez.

Off the 122 invertebrate taxa recorded on transects during our study, the vast majority (> 80%) of those with documented distributions were restricted to the southeast Atlantic,

southeast Pacific, sub-Antarctic, and Antarctic regions. The combination of the unique oceanographic conditions and heterogeneity in the Chilean coast has resulted in high levels of endemism in many invertebrate groups, with several marine invertebrate taxa showing latitudinal biodiversity patterns, some explained by the presence of Antarctic fauna [27]. The Chilean fjord region is diverse in terms of marine invertebrate fauna but also poorly studied [81], and our study is therefore important in better understanding the biogeography of the region and establishing baselines for future studies.

Unlike kelp forests in other regions of the world, the fish assemblages in the Magellan Region are not a conspicuous component of the community [82]. The nearshore fishes of southern Chile form a distinct biogeographic unit that extends towards the Atlantic, including the Falkland Islands [83]. The number of fish species and species composition that we observed was low but similar to that of a two-year study conducted by Moreno and Jara [82] at Puerto Toro on Navarino Island, just south of the Beagle Channel. Richness of littoral fishes on the Chilean coast shows a progressive decrease toward higher latitudes, with a marked decrease of species south of 40° S [68,84]. This observed pattern is likely due to the absence of species of subtropical origin, primarily herbivorous fishes, as well as the lack of time for these species to have colonized, evolved, and adapted to colder temperatures following the last glaciation [85]. Of the 49 species of fishes reported from the Beagle Channel to 150 m, 67% are endemic to the Magellanic Province [86], and our results are consistent with this, where as 83% of the shallow-water fish species that we observed were endemic to the Magellanic Province.

A recent meta-analysis of global marine biodiversity showed that fish abundance declined steeply toward polar latitudes, whereas invertebrate abundance trended in the opposite direction [87]. These authors suggest that temperature-mediated metabolic rate-dependent mechanisms favored fishes in tropical regions, with fish predation and herbivory constraining mobile macroinvertebrate diversity at these lower latitudes. Conversely, invertebrate richness increased with increases in nutrients and a decrease in the abundance of predatory fishes.

The shallow fish fauna in the region was dominated by the suborder Notothenioidei (cod icefish), represented by the families Bovichtidae, Eleginopsidae, Nototheniidae, Harpagiferidae and Channichthyidae [82,84,86]. These fishes play a key role in the ecosystem, occupying most of the available trophic niches [88–89], although dominated by detritivores that fed primarily on amphipods and isopods associated with the kelp [82]. They are also important prey for sea lions, cormorants (*Phalacrocorax atriceps*), and the magellanic penguin [90–92] that frequent the area.

Examination of mesophotic depths (53–105 m) revealed a diverse assemblage of species. On the rocky slopes and boulder habitat, echinoderms, mollusks, bryozoans, and sponges were abundant. The fjord region is a dynamic mixing zone, resulting from deep-water emergence, where typically deep-water organisms can be found in comparably shallow water [81]. The deep and mid-depth species mix, resulted in novel communities in the fjord region. Furthermore, there is an east-west gradient in species composition, where close to the continent, the glacial silt habitat supports a high biomass of scavengers and predators (sharks and rays). In these habitats, we saw that the scavenging southern hagfish was the most abundant fish encountered on our deployments. Because of the barriers to dispersal, and the dynamic environment, the deep Chilean fjords represent a unique mixing zone of species, with high biodiversity value.

Overfishing has severely impacted the stocks of Patagonian toothfish, southern hake, and king crab, which are the major economic driver of the region [36]. These fisheries previously provided a much greater contribution to the local economy and employment, but declining

stocks have caused severe economic hardships and social displacements. Continued fishing at these levels will only hasten the collapse of these important resources.

Climate-mediated changes are occurring to kelp forests worldwide due to increases in temperature, explosions of sea urchin populations, and overfishing, which can act synergistically to exacerbate kelp declines [93–94]. Kelps dominate cold-water coastal zones and can become physiologically stressed at high sea temperatures, particularly when nutrient availability is low [95–96]. However, the Humboldt Current is the only boundary current that is not currently showing signs of tropicalization [93], and this region may therefore be less impacted by climate change compared with kelp forests elsewhere around the world.

While the tropicalization of this region is currently a lower priority threat to these ecosystems, human mediated introductions of exotic aquaculture species present a more immediate concern. From the 1970s to 1990s, efforts to introduce exotic salmonids in Chile were focused on ocean ranching with the intent to establishing wild populations of Chinook salmon (*Oncorhynchus tshawytscha*) in Chiloé Island and the Prat River in the Última Esperanza Fjord (Magellan Region) [97–98]. The industry is currently expanding into the Aysén and Magellan regions, and one of the main reasons for this expansion to more isolated and cooler areas was a large-scale outbreak of an infectious salmon anemia virus between 2008 and 2010 around Chiloé Island [99].

Chinook salmon have invaded nearly the entire Patagonia region [99], constituting a major threat to biodiversity to the area [100]. They have been confirmed reports of Chinook spawning in rivers off the Beagle Channel, and the establishment of spawning populations has the potential to severely impact native fishes and invertebrate populations throughout the region [101]. The observed diet in escaped salmonids includes fishes, crustaceans, insects and molluscs [97,100], likely imposing a strong predatory pressure on schooling fishes and increasing resource competition with native fishes [100,102–104]. By some estimates, if current escape rates are not reduced, escaped salmon may exceed 4.4 million individuals per year, consuming up to 6600 t of pelagic prey [98]. In addition, the copious amounts of feces, unconsumed feed, and dead fish greatly increase the nutrient load into fjords and other sheltered areas with poor circulation, resulting in lethal consequences to the benthic communities associated with these salmon net pens [81]. The introduction of antibiotics, pesticides, and other pharmaceuticals are also concerns associated with salmon farms in the region. The expansion of this industry, with a long history of environmental impact in Chile [105–106] represents a threat to the biodiversity and conservation of the entire ecosystem of the Magellan region.

The Humboldt Current ecosystem remains largely unprotected [107–109]. The islands in Cape Horn and Diego Ramírez and the waters surrounding them are at a key moment due to increasing local and global stressors. The Chilean Government has declared a marine park that would include Diego Ramírez to the southern limits of the exclusive economic zone of Chile. This would protect >100,000 km², and not only help conserve kelp forests, but also essential habitat for important populations of sea lions, sea elephants, dolphins, whales, penguins, petrels, albatrosses and other seabirds. The prohibition of fishing in this large area would help recover stocks of southern hake, southern king crab and Patagonian toothfish, which have been severely overfished in the region, as well as reduce by-catch of albatrosses, rays, sharks and other vulnerable species. Krill and sardines are the base of the entire food web of the region, and their protection would increase the health of the entire ecosystem. The Diego Ramírez and Cape Horn archipelagos are likely connected to southern South America via the West Wind Drift [73,110–111], and protecting this connectivity is key to the sustainability the ecosystem. This large protected area is an essential step in conserving the biodiversity and ecosystem functioning of the entire region.

Supporting information

S1 Table. Invertebrate taxa recorded during shallow (< 20 m) scuba surveys. Func.

Grp. = Functional feeding groups: 1—passive suspension feeder, 2—active suspension feeder, 3—herbivorous/browser, 4—carnivore, 5—omnivore, and 6—deposit feeder.

(DOCX)

S2 Table. Taxa observed on deep sea Drop-cams.

(DOCX)

Acknowledgments

We would like to thank the Chilean Navy for sponsoring this expedition, especially to Commander Andrés Rodrigo for advice and guidance in planning, as well as the support provided by the Tercera Zona Naval. We would also like to express our gratitude for the support provided by Governor Jorge Flies of the Magellan and Chilean Antarctic Region, along with the Minister of the Environment Marcelo Mena, the former Minister of the Environment Pablo Badenier, and Alejandra Figueroa, the director of the Natural Resources and Biodiversity Division. Additionally, we would like to acknowledge and thank the captain and crew of the M/Y Plan B and the Waitt Foundation for providing the platform for this expedition, as well as their tirelessly work to help make the expedition a success. Finally, we wish to thank and congratulate the President of Chile, Michelle Bachelet, for her leadership in the conservation of Chile's ocean and in her decision to protect the waters around Cabo de Hornos and Diego Ramírez islands to the southern end of the zone economic zone of Chile.

Author Contributions

Conceptualization: Alan M. Friedlander, Enric Ballesteros, Mathias Hüne, Alex Muñoz, Enric Sala.

Data curation: Alan M. Friedlander, Enric Ballesteros, Brad Henning, Mathias Hüne, Pelayo Salinas-de-León.

Formal analysis: Alan M. Friedlander, Enric Ballesteros, Tom W. Bell, Jonatha Giddens, Mathias Hüne, Pelayo Salinas-de-León.

Funding acquisition: Enric Sala.

Investigation: Alan M. Friedlander, Enric Ballesteros, Tom W. Bell, Mathias Hüne, Alex Muñoz, Pelayo Salinas-de-León.

Methodology: Alan M. Friedlander, Enric Ballesteros, Tom W. Bell, Jonatha Giddens, Brad Henning, Mathias Hüne, Pelayo Salinas-de-León.

Project administration: Alan M. Friedlander, Alex Muñoz, Enric Sala.

Resources: Alan M. Friedlander, Enric Ballesteros, Tom W. Bell, Brad Henning, Mathias Hüne, Pelayo Salinas-de-León, Enric Sala.

Software: Alan M. Friedlander, Enric Ballesteros, Tom W. Bell, Jonatha Giddens, Pelayo Salinas-de-León.

Supervision: Alan M. Friedlander, Alex Muñoz, Enric Sala.

Validation: Alan M. Friedlander, Enric Ballesteros, Brad Henning, Mathias Hüne, Pelayo Salinas-de-León.

Visualization: Alan M. Friedlander, Tom W. Bell, Pelayo Salinas-de-León.

Writing – original draft: Alan M. Friedlander, Tom W. Bell.

Writing – review & editing: Alan M. Friedlander, Enric Ballesteros, Tom W. Bell, Jonatha Giddens, Brad Henning, Mathias Hüne, Alex Muñoz, Pelayo Salinas-de-León, Enric Sala.

References

1. Dayton PK. Experimental evaluation of ecological dominance in a rocky intertidal algal community. *Ecol Monogr.* 1975; 45(2):137–159.
2. Steneck RS, Graham MH, Bourque BJ, Corbett D, Erlandson JM, Estes JA, et al. Kelp forest ecosystems: biodiversity, stability, resilience and future. *Environ Conser.* 2002; 29(4):436–459.
3. Arkema KK, Reed DC, Schroeter SC. Direct and indirect effects of giant kelp determine benthic community structure and dynamics. *Ecology.* 2009; 90(11):3126–37. PMID: [19967868](https://pubmed.ncbi.nlm.nih.gov/19967868/)
4. Steneck RS, Johnson CR. Kelp forests: dynamic patterns, processes, and feedbacks. In: Bertness MD, Bruno JF, Silliman BR, Stachowicz JJ, editors. *Marine Community Ecology and Conservation*. Sunderland, MA: Sinauer Associates, Inc.; 2014. pp. 315–336.
5. Mann KH. Seaweeds: their productivity and strategy for growth. *Science.* 1973; 182(4116):975–81. <https://doi.org/10.1126/science.182.4116.975> PMID: [17833778](https://pubmed.ncbi.nlm.nih.gov/17833778/)
6. Dayton PK. Ecology of kelp communities. *Annu Rev Ecol Evol Syst.* 1985; 16(1):215–45.
7. Graham MH, Vasquez JA, Buschmann AH. Global ecology of the giant kelp *Macrocystis*: from ecotypes to ecosystems. In: Gibson RN, Atkinson JD, Gordon JDM, editors. *Oceanography and Marine Biology: An Annual Review Volume 45*. Boca Raton, FL: CRC Press; 2007. pp. 39–88.
8. Reed DC, Rassweiler A, Arkema KK. Biomass rather than growth rate determines variation in net primary production by giant kelp. *Ecology.* 2008; 89(9):2493–505. PMID: [18831171](https://pubmed.ncbi.nlm.nih.gov/18831171/)
9. Holbrook SJ, Carr MH, Schmitt RJ, Coyer JA. Effect of giant kelp on local abundance of reef fishes: the importance of ontogenetic resource requirements. *Bull Mar Sci.* 1990; 47(1):104–114.
10. Reed DC, Rassweiler A, Carr MH, Cavanaugh KC, Malone DP, Siegel DA. Wave disturbance overwhelms top-down and bottom-up control of primary production in California kelp forests. *Ecology.* 2011; 92(11):2108–2116. PMID: [22164835](https://pubmed.ncbi.nlm.nih.gov/22164835/)
11. Young M, Cavanaugh K, Bell T, Raimondi P, Edwards CA, Drake PT, et al. Environmental controls on spatial patterns in the long-term persistence of giant kelp in central California. *Ecol Monogr.* 2016; 86(1):45–60.
12. Bell TW, Cavanaugh KC, Reed DC, Siegel DA. Geographical variability in the controls of giant kelp biomass dynamics. *J Biogeogr.* 2015; 42(10):2010–2021.
13. Estes JA, Duggins DO. Sea otters and kelp forests in Alaska: generality and variation in a community ecological paradigm. *Ecol Monogr.* 1995; 65(1):75–100.
14. Foster MS, Schiel DR. Loss of predators and the collapse of southern California kelp forests (?): alternatives, explanations and generalizations. *J Exp Mar Biol Ecol.* 2010; 393(1):59–70.
15. Pérez-Matus A, Carrasco SA, Gelcich S, Fernandez M, Wieters EA. Exploring the effects of fishing pressure and upwelling intensity over subtidal kelp forest communities in Central Chile. *Ecosphere.* 2017; 8(5):e01808.
16. Dayton PK, Tegner MJ, Edwards PB, Riser KL. Sliding baselines, ghosts, and reduced expectations in kelp forest communities. *Ecol Appl.* 1998; 8(2):309–22.
17. Graham MH. Effects of local deforestation on the diversity and structure of southern California giant kelp forest food webs. *Ecosystems.* 2004; 7(4):341–57.
18. Estes JA, Terborgh J, Brashares JS, Power ME, Berger J, Bond WJ, et al. Trophic downgrading of planet Earth. *Science.* 2011; 333(6040):301–306. <https://doi.org/10.1126/science.1205106> PMID: [21764740](https://pubmed.ncbi.nlm.nih.gov/21764740/)
19. Frank KT, Petrie B, Choi JS, Leggett WC. Trophic cascades in a formerly cod-dominated ecosystem. *Science.* 2005; 308(5728):1621–1623. <https://doi.org/10.1126/science.1113075> PMID: [15947186](https://pubmed.ncbi.nlm.nih.gov/15947186/)
20. Rabassa J, Coronato A, Bujalesky G, Salemme M, Roig C, Meglioli A, et al. Quaternary of Tierra del Fuego, southernmost South America: an updated review. *Quat Int.* 2000; 68:217–40.
21. Veblen TT, Hill RS, Read J. *The Ecology and Biogeography of Nothofagus Forests*. New Haven: Yale University Press; 1996.
22. Silander JA Jr. Temperate forests: plant species biodiversity and conservation. In: Levin SA, editor. *Encyclopedia of biodiversity*, vol. 5. New York, NY: Academic Press; 2000. pp. 607–626.

23. Rozzi R, Armesto JJ, Gutiérrez JR, Massardo F, Likens GE, Anderson CB, et al. Integrating ecology and environmental ethics: earth stewardship in the southern end of the Americas. *BioScience*. 2012; 62(3):226–36.
24. King PP. Some observations upon the geography of the southern extremity of South America, Tierra del Fuego, and the Strait of Magalhaens. *J Royal Geogr Soc London*. 1831; 1:155–175.
25. Zappettini EO, Mendía J. The first geological map of Patagonia. Darwin in Argentina. *Rev Asoc Geol Argent*. 2009; 64(1):55e59.
26. Fernández M, Jaramillo E, Marquet PA, Moreno CA, Navarrete SA, Ojeda FP, et al. Diversity, dynamics and biogeography of Chilean benthic nearshore ecosystems: an overview and guidelines for conservation. *Rev Chil Hist Nat*. 2000; 73(4):797–830.
27. Miloslavich P, Klein E, Díaz JM, Hernández CE, Bigatti G, Campos L, et al. Marine Biodiversity in the Atlantic and Pacific Coasts of South America: Knowledge and Gaps. *PLoS ONE*. 2011; 6(1):e14631. <https://doi.org/10.1371/journal.pone.0014631> PMID: 21304960
28. Aguayo-Lobo A, Acevedo J, Brito JL, Olavarria C, Moraga R, Olave C. The southern right whale, *Eubalaena australis* (Desmoulins, 1822) in Chilean waters: analysis of records from 1976–2008. *J Mar Biol Ocean*. 2008; 43(3):653–668.
29. Acevedo J, Rasmussen K, Felix FE, Castro C, Llano M, Secchi E, et al. Migratory destinations of humpback whales from the Magellan Strait feeding ground, Southeast Pacific. *Mar Mamm Sci*. 2007; 23(2):453–63.
30. Falabella V, Campagna C, Croxall J. Atlas del Mar Patagónico: Especies y Espacios. Buenos Aires, Argentina: Wildlife Conservation Society and BirdLife International; 2009.
31. Vila AR, Falabella VA, Gálvez M, Farías A, Droguett D, Saavedra B. Identifying high-value areas to strengthen marine conservation in the channels and fjords of the southern Chile ecoregion. *Oryx*. 2016; 50(2):1–9.
32. Darwin CR. Narrative of the surveying voyages of His Majesty's Ships Adventure and Beagle between the years 1826 and 1836, describing their examination of the southern shores of South America, and the Beagle's circumnavigation of the globe. Journal and remarks. 1832–1836. London: Henry Colburn; 1839.
33. Hidalgo J, Schiappacasse V, Niemeyer H, Aldunate C, Mege P. Etnografía: Sociedades Indígenas Contemporáneas y Su Ideología. Santiago: Editorial Andrés Bello; 1996.
34. McEwan C, Borrero L, Prieto A. Patagonia: Natural History, Prehistory and Ethnography at the Uttermost Part of the Earth. Princeton, NJ: Princeton University Press; 1997.
35. Moran E. Indigenous South Americans of the past and present: an ecological perspective. *J Roy Anthropol Inst*. 2000; 6(3):534–534.
36. Pollack G, Berghöfer A, Berghöfer U. Fishing for social realities—Challenges to sustainable fisheries management in the Cape Horn Biosphere Reserve. *Mar Policy*. 2008; 32(2):233–242.
37. Alheit J, Pitcher TJ. Hake: biology, fisheries and markets, 2nd ed. Berlin: Springer Science & Business Media; 2012.
38. Henríquez V, Licandeo R, Cubillos LA, Cox SP. Interactions between ageing error and selectivity in statistical catch-at-age models: simulations and implications for assessment of the Chilean Patagonian toothfish fishery. *ICES J Mar Sci*. 2016; 73(4):1074–1090.
39. Vasquez JA, Buschmann A. Herbivore-kelp interactions in Chilean subtidal communities: a review. *Rev Chil Hist Nat*. 1997; 70:41–52.
40. Rozzi R, Massardo F, Anderson C, Heidinger K, Silander J Jr. Ten principles for biocultural conservation at the southern tip of the Americas: the approach of the Omora Ethnobotanical Park. *Ecology and Society*. 2006; 11(1):43.
41. Haro D, Aguayo-Lobo A, Acevedo J. Características oceanográficas y biológicas de las comunidades del plankton y nekton del Área Marina Costera Protegida Francisco Coloane: Una revisión. *An Inst Patagonia*. 2013; 41:77–90.
42. Cabezas A. Área Marina y Costera Protegida de Múltiples Usos Francisco Coloane. In: de Chile Gobierno, editor. Conservación de la biodiversidad de importancia mundial a lo largo de la costa chilena. Santiago: Ocho Libros Editores; 2007. pp. 136–139.
43. Antezana T. Hydrographic features of Magellan and Fuegian inland passages and adjacent Subantarctic waters. *Sci Mar*. 1999; 63(S1):23–34.
44. Guglielmo L, Antezana T, Costanzo G, Zagami G. Zooplankton communities in the Straits of Magellan. *Mem Biol Mar Ocean*. 1991; 19:157–161.
45. Ríos C, Mutschke E, Morrison E. Biodiversidad bentónica sublitoral en el estrecho de Magallanes, Chile. *Rev Biol Mar Oceanogr*. 2003 Jul; 38(1):1–2.

46. Cunningham SA, Alderson SG, King BA, Brandon MA. Transport and variability of the Antarctic circumpolar current in Drake passage. *J Geophys Res: Oceans*. 2003; 108(C5).
47. Clark AH. *The Clipper Ship Era: An Epitome of Famous American and British Clipper Ships, Their Owners, Builders, Commanders, and Crews, 1843–1869*. New York: GP Putnam's Sons; 2011.
48. Rydell RA. *Cape Horn to the Pacific: the rise and decline of an ocean highway*. Berkeley: University of California Press; 1952.
49. Bernstein WJ. *A splendid exchange: How trade shaped the world*. New York: Atlantic Monthly Press; 2009.
50. Fleming DK. Patterns of international ocean trade. In: Grammenos CTH, editor. *The Handbook of Maritime Economics and Business*. London: Informa Law; 2002. pp.63–89.
51. Callicott JB, Rozzi R, Delgado L, Monticino M, Acevedo M, Harcombe P. Biocomplexity and conservation of biodiversity hotspots: three case studies from the Americas. *Philos Trans R Soc Lond B Biol Sci*. 2007; 362(1478):321–333. <https://doi.org/10.1098/rstb.2006.1989> PMID: 17255039
52. Rozzi R, Armesto JJ, Goffinet B, Buck W, Massardo F, Silander J, et al. Changing lenses to assess biodiversity: patterns of species richness in sub-Antarctic plants and implications for global conservation. *Front Ecol Environ*. 2008; 6(3):131–137.
53. Kirkwood R, Lawton K, Moreno C, Valencia J, Schlatter R, Robertson G. Estimates of southern rockhopper and macaroni penguin numbers at the Idefonso and Diego Ramírez Archipelagos, Chile, using quadrat and distance-sampling techniques. *Waterbirds*. 2007; 30(2):259–267.
54. Robertson G, Moreno C, Arata JA, Candy SG, Lawton K, Valencia J, et al. Black-browed albatross numbers in Chile increase in response to reduced mortality in fisheries. *Biol Cons*. 2014; 169:319–333.
55. Roberts DA, Gardner M, Church R, Ustin S, Scheer G, Green RO. Mapping chaparral in the Santa Monica Mountains using multiple endmember spectral mixture models. *Remote Sens Environ*. 1998; 65(3):267–279.
56. Cavanaugh KC, Siegel DA, Reed DC, Dennison PE. Environmental controls of giant kelp biomass in the Santa Barbara Channel, California. *Mar Ecol Prog Ser*. 2011; 429:1–17.
57. Hepburn CD, Hurd C. Conditional mutualism between the giant kelp *Macrocystis pyrifera* and colonial epifauna. *Mar Ecol Prog Ser*. 2005; 302:37–48.
58. Bell TW, Cavanaugh KC, Reed DC, Siegel DA. Geographical variability in the controls of giant kelp biomass dynamics. *J Biogeogr*. 2015; 42:2010–2021.
59. Bell TW, Cavanaugh KC, Siegel DA. Remote monitoring of giant kelp biomass and photosynthetic condition: An evaluation of the potential for the Hyperspectral Infrared Imager (HypSIIRI) mission. *Remote Sens Environ*. 2015; 167:218–228.
60. Tissot BN, Hixon MA, Stein DL. Habitat-based submersible assessment of macro-invertebrate and groundfish assemblages at Heceta Bank, Oregon, from 1988 to 1990. *J Exp Mar Bio Ecol*. 2007; 352(1):50–64.
61. Zar JH. *Biostatistical analysis*, 5th edition. New Jersey: Prentice-Hall, Inc.; 2007.
62. Ludwig JA, Reynolds JF. *Statistical Ecology*. New York, New York: John Wiley and Sons; 1998.
63. Pielou EC. *Mathematical Ecology*. New York: John Wiley & Sons; 1977.
64. Froese R, Pauly D, 2012. FishBase. [cited 2017, Nov 26]. WWW.Fishbase.org.
65. Anderson MJ, Gorley RN, Clarke KR. PERMANOVA+ for PRIMER: Guide to Software and Statistical Methods. Plymouth, UK. PRIMER-E, 2008.
66. Clarke KR. Non-parametric multivariate analyses of changes in community structure. *Aust J Ecol*. 1993; 18:117–143.
67. Ríos C, Arntz WE, Gerdes D, Mutschke E, Montiel A. Spatial and temporal variability of the benthic assemblages associated to the holdfasts of the kelp *Macrocystis pyrifera* in the Straits of Magellan, Chile. *Polar Biol*. 2007; 31(1):89–100.
68. Ojeda FP, Labra FA, Muñoz AA. Biogeographic patterns of Chilean littoral fishes. *Rev Chil Hist Nat*. 2000; 73(4):625–641.
69. Cañete JI, Díaz-Ochoa JA, Figueroa T, Medina A. Infestation of *Pseudione tuberculata* (Isopoda: Bopyridae) on juveniles of *Lithodes santolla* (Magellan region, Chile): a spatial mesoscale analysis. *Lat Am J Aquat Res*. 2017; 45(1):79–93.
70. Ling SD, Scheibling RE, Rassweiler A, Johnson CR, Shears N, Connell SD, et al. Global regime shift dynamics of catastrophic sea urchin overgrazing. *Phil Trans R Soc B*. 2015; 370(1659):20130269.
71. Estes JA, Palmisano JF. Sea otters: their role in structuring nearshore communities. *Science*. 1974; 185(4156):1058–1060. <https://doi.org/10.1126/science.185.4156.1058> PMID: 17738247

72. Jackson JB, Kirby MX, Berger WH, Bjorndal KA, Botsford LW, Bourque BJ, et al. Historical overfishing and the recent collapse of coastal ecosystems. *Science*. 2001; 293(5530):629–637. <https://doi.org/10.1126/science.1059199> PMID: 11474098
73. Dayton PK. The structure and regulation of some South American kelp communities. *Ecol Monog*. 1985; 55(4):447–68.
74. Vasquez JA, Castilla JC, Santelices B. Distributional patterns and diets of four species of sea urchins in giant kelp forest (*Macrocystis pyrifera*) of Puerto Toro, Navarino Island, Chile. *Mar Ecol Prog Ser*. 1984; 19:55–63
75. Castilla JC. Food webs and functional aspects of the kelp, *Macrocystis pyrifera*, community in the Beagle Channel, Chile. In: Siegfried WR, Condy PR, Laws RM, editors. *Antarctic Nutrient Cycles and Food Webs*. Berlin: Springer-Verlag; 1985. pp. 407–414.
76. Castilla JC, Moreno CA. 1982. Sea urchins and *Macrocystis pyrifera*: experimental test of their ecological relations in southern Chile. In: Lawrence JM, editor. *Proceedings of the International Echinoderm Conference*. Rotterdam, The Netherlands: AA Balkema. pp. 257–263.
77. Santelices B, Ojeda FP. Population dynamics of coastal forests *Macrocystis pyrifera* in Puerto Toro, Isla Navarino, Southern Chile. *Mar Ecol Prog Ser*. 1984; 14(2):175–83.
78. Buschmann AH. Estructura y organizacion de ensambles de macroalgas en mares interiores del sur de Chile. Ph.D. Thesis, Facultad de Ciencias Biologicas, Pontificia Universidad Catolica de Chile. 1995.
79. Vásquez J, Castilla JC. Some aspects of the biology and trophic range of *Cosmasterias lurida* (Asteroidea, Asteroiinae) in belts of *Macrocystis pyrifera* at Puerto Toro, Chile. *Medio Ambiente*. 1984; 7(1):47–51.
80. Castilla JC, Guiñez R. Disjoint geographical distribution of intertidal and nearshore benthic invertebrates in the Southern Hemisphere. *Rev Chil Hist Nat*. 2000; 73(4):585–603.
81. Häussermann V, Försterra G. Marine benthic fauna of Chilean Patagonia. Santiago: Nature in Focus; 2009.
82. Moreno CA, Jara HF. Ecological studies on fish fauna associated with *Macrocystis pyrifera* belts in the south of Fuegian Islands, Chile. *Mar Ecol Prog Ser*. 1984; 15:99–107.
83. Pequeño G. Peces del crucero CIMAR-Fiordo 2, a los canals patagónicos de Chile, consideraciones ictiogeográficas. *Cienc Tecnol Mar* 1999; 22:165–179.
84. Navarrete AH, Lagos NA, Ojeda P. Latitudinal diversity patterns of Chilean coastal fishes: searching for casual processes. *Rev Chil Hist Nat*. 2014; 87:2.
85. Mead GW. A history of South Pacific fishes. In: Wooster WS, editor. *Scientific exploration of the South Pacific*. Washington DC: National Academy of Sciences; 1970. pp 236–251.
86. Lloris D, Rucabado J. Ictiofauna del Canal Beagle (Tierra del Fuego), aspectos ecológicos y análisis biogeográfico. Madrid: Instituto Español de Oceanografía; 1991. ISBN: 8474798965.
87. Edgar GJ, Alexander TJ, Lefcheck JS, Bates AE, Kininmonth SJ, Thomson RJ, et al. Abundance and local-scale processes contribute to multi-phyla gradients in global marine diversity. *Sci Adv*. 2017; 3(10):e1700419. <https://doi.org/10.1126/sciadv.1700419> PMID: 29057321
88. Hüne M, Ojeda J. Estructura del ensamble de peces costeros de los canals y fiordos de la zona central de la Patagonia chilena (48°–52° S). *Rev Biol Mar Oceanogr*. 2012; 47:451–460.
89. Hüne M, Vega R. Spatial variation in the diet of *Patagonotothen tessellate* (Pisces, Nototheniidae) from the fjords and channels of southern Chilean Patagonia. *Polar Biol*. 2015; 38:1613–1622.
90. Boswall J, MacIver D. The magellanic penguin *Spheniscus magellanicus*. In: Stonehouse B, editor. *The Biology of penguins*. London: Macmillian; 1975. pp. 271–305.
91. Casaux R, Barrera-Oro E. Shags in Antarctica: their feeding behaviour and ecological role in the marine food web. *Antarct Sci*. 2006; 18(1):3–14.
92. Casaux R, Baroni A, Ramon A. Diet of antarctic fur seals *Arctocephalus gazella* at the Danco Coast, Antarctic Peninsula. *Polar Biol*. 2003; 26(1):49–54.
93. Vergés A, Steinberg PD, Hay ME, Poore AG, Campbell AH, Ballesteros E, et al. The tropicalization of temperate marine ecosystems: climate-mediated changes in herbivory and community phase shifts. *Phil Trans R Soc B*. 2014; 281(1789):20140846.
94. Krumhansl KA, Okamoto DK, Rassweiler A, Novak M, Bolton JJ, Cavanaugh KC, et al. Global patterns of kelp forest change over the past half-century. *Proc Natl Acad Sci USA*. 2016; 113(48):13785–13790. <https://doi.org/10.1073/pnas.1606102113> PMID: 27849580
95. Tegner MJ, Basch LV, Dayton PK. Near extinction of an exploited marine invertebrate. *Trends in Ecology & Evolution*. 1996; 11(7):278–280.

96. Gerard VA. The role of nitrogen nutrition in high-temperature tolerance of kelp, *Laminaria saccharina*. *J Phycol.* 1997; 33:800–810.
97. Soto D, Jara F, Moreno C. Escaped salmon in the inner seas, Southern Chile: facing ecological and social conflicts. *Ecol Appl.* 2001; 11:1750–1762.
98. Niklitschek EJ, Soto D, Lafon A, Molinet C, Toledo P. Southward expansion of the Chilean salmon industry in the Patagonian Fjords: main environmental challenges. *Rev Aquacult.* 2013; 5(3):172–195.
99. Mardones FO, Perez AM, Carpenter TE. Epidemiologic investigation of the re-emergence of infectious salmon anemia virus in Chile. *Dis Aquat Org.* 2009; 84(2):105–14. <https://doi.org/10.3354/dao02040> PMID: 19476280
100. Ciancio JE, Pascual MA, Botto F, Frere E, Iribarne O. Trophic relationships of exotic anadromous salmonids in the southern Patagonian Shelf as inferred from stable isotopes. *Limnol Oceanogr.* 2008; 53(2):788–98.
101. Soto D, Arismendi I, Di Prinzio C, Jara F. Establishment of Chinook salmon (*Oncorhynchus tshawytscha*) in Pacific basins of southern South America and its potential ecosystem implications. *Rev Chil Hist Nat.* 2007; 80(1):81–98.
102. Fernández DA, Ciancio J, Ceballos SG, Riva-Rossi C, Pascual MA. Chinook salmon (*Oncorhynchus tshawytscha*, Walbaum 1792) in the Beagle Channel, Tierra del Fuego: the onset of an invasion. *Biol Invasions.* 2010; 12(9):2991–2997.
103. Ciancio J, Beauchamp DA, Pascual M. Marine effect of introduced salmonids: prey consumption by exotic steelhead and anadromous brown trout in the Patagonian Continental Shelf. *Limnol Oceanogr.* 2010; 55(5):2181–2192.
104. Riccialdelli L, Newsome SD, Fogel ML, Fernández DA. Trophic interactions and food web structure of a subantarctic marine food web in the Beagle Channel: Bahía Lapataia, Argentina. *Polar Biol.* 2017; 40(4):807–21.
105. Asche F, Hansen H, Tveterås R, Tveterås S. The salmon disease crisis in Chile. *Mar Resour Econ.* 2009; 24(4):405–411.
106. Buschmann AH, Cabello F, Young K, Carvajal J, Varela DA, Henríquez L. Salmon aquaculture and coastal ecosystem health in Chile: analysis of regulations, environmental impacts and bioremediation systems. *Ocean Coast Manag.* 2009; 52(5):243–249.
107. Thiel M, Macaya EC, Acuna E, Arntz WE, Bastias H, Brokordt K, et al. The Humboldt Current System of northern and central Chile: oceanographic processes, ecological interactions and socioeconomic feedback. In: Gibson RN, Atkinson JD, Gordon JDM, editors. *Oceanography and Marine Biology: An Annual Review Volume 45.* 2007. pp. 195–344.
108. Tognelli MF, Fernández M, Marquet PA. Assessing the performance of the existing and proposed network of marine protected areas to conserve marine biodiversity in Chile. *Biol Conserv.* 2009; 142(12):3147–3153.
109. Guarderas AP, Hacker SD, Lubchenco J. Current status of marine protected areas in Latin America and the Caribbean. *Conserv Biol.* 2008; 22(6):1630–1640. <https://doi.org/10.1111/j.1523-1739.2008.01023.x> PMID: 18717690
110. Pequeño G. Comments on fishes from the Diego Ramírez Islands, Chile. *Jpn J Ichthyol.* 1986; 32(4):440–442.
111. Waters JM. Driven by the West Wind Drift? A synthesis of southern temperate marine biogeography, with new directions for dispersalism. *J Biogeogr.* 2008; 35(3):417–427.

S1 Table. Invertebrate taxa recorded during shallow (< 20 m) scuba surveys. Func. Grp. = Functional feeding groups: 1 – passive suspension feeder, 2 - active suspension feeder, 3 - herbivorous/browser, 4 - carnivore, 5 -omnivore, and 6 - deposit feeder.

Phylum	Class to Infraclass	Order to Family	Func. Grp	Taxa
Annelida	Polychaeta	Serpulidae	2	<i>Apomatus</i> sp.
Annelida	Polychaeta	Chaetopteridae	2	<i>Chaetopterus variopedatus</i>
Arthropoda	Hexanauplia	Balanidae	2	<i>Arossia henryae</i>
Arthropoda	Hexanauplia	Balanidae	2	<i>Austromegabalanus psittacus</i>
Arthropoda	Hexanauplia	Balanidae	2	<i>Balanus</i> cf. <i>laevis</i>
Arthropoda	Hexanauplia	Archaeobalanidae	2	<i>Notobalanus flosculus</i>
Arthropoda	Malacostraca	Munididae	5	<i>Munida gregaria</i>
Arthropoda	Malacrostaca	Campylonotidae	4	<i>Campylonotus vagans</i>
Arthropoda	Malacrostaca	Inachidae	4	<i>Eurypodius latreillii</i>
Arthropoda	Malacrostaca	Hymenosomatidae	4	<i>Halicarcinus planatus</i>
Arthropoda	Malacrostaca	Lithodidae	4	<i>Lithodes santolla</i>
Arthropoda	Malacrostaca	Hippolytidae	4	<i>Nauticaris magellanica</i>
Arthropoda	Malacrostaca	Paguridae	4	<i>Pagurus comptus</i>
Arthropoda	Malacrostaca	Lithodidae	4	<i>Paralomis granulosa</i>
Arthropoda	Malacrostaca	Trichopeltariidae	4	<i>Peltarion spinulosum</i>
Arthropoda	Pycnogonida	Pycnogonidae	4	Pycnogonidae
Brachiopoda	Rhynchonellata	Terebratellidae	2	<i>Magellania venosa</i>
Bryozoa	Gymnolaemata	Beaniidae	2	<i>Beania magellanica</i>
Bryozoa	Gymnolaemata	Bugulidae	2	<i>Bugula</i> sp.
Bryozoa	Gymnolaemata	Cellariidae	2	<i>Cellaria malvinensis</i>
Bryozoa	Gymnolaemata	Microporellidae	2	<i>Microporella hyadesi</i>
Bryozoa	Gymnolaemata	Bitectiporidae	2	<i>Schizomavella</i> sp.
Bryozoa	Stenolaemata	Crisiidae	2	<i>Crisia</i> sp.
Bryozoa	Stenolaemata	Entalophoridae	2	<i>Entalophora</i> sp.
Bryozoa			2	Unid. encrusting small bryozoa
Bryozoa			2	Unid. encrusting thin bryozoan
Bryozoa			2	Unid. <i>Schizobrachiella</i> -like
Chordata	Ascidiacea	Polyclinidae	2	<i>Aplidium fuegiense</i>
Chordata	Ascidiacea	Polyclinidae	2	<i>Aplidium magellanicum</i>
Chordata	Ascidiacea	Polyclinidae	2	<i>Aplidium</i> sp. 1
Chordata	Ascidiacea	Polyclinidae	2	<i>Aplidium</i> sp. 2

S1 Table. Continued.

Phylum	Class to Infraclass	Order to Family	Func. Grp	Taxa
Chordata	Ascidiacea	Styelidae	2	<i>Cnemidocarpa sp.</i>
Chordata	Ascidiacea	Styelidae	2	<i>Cnemidocarpa verrucosa</i>
Chordata	Ascidiacea	Corellidae	2	<i>Corella eumyota</i>
Chordata	Ascidiacea	Didemnidae	2	<i>Didemnum studeri</i>
Chordata	Ascidiacea	Styelidae	2	<i>Polyzoa opuntia</i>
Chordata	Ascidiacea	Pyuridae	2	<i>Pyura chilensis</i>
Chordata	Ascidiacea	Pyuridae	2	<i>Pyura legumen</i>
Chordata	Ascidiacea	Holozoidae	2	<i>Sycozoa gaimardi</i>
Cnidaria	Anthozoa	Isophelliidae	1	<i>Acontiaria sp.</i>
Cnidaria	Anthozoa	Actiniaria	1	Actiniaria
Cnidaria	Anthozoa	Actinostolidae	1	<i>Actinostola chilensis</i>
Cnidaria	Anthozoa	Alcyoniidae	1	<i>Alcyonium cf. yepayek</i>
Cnidaria	Anthozoa	Actinostolidae	1	<i>Antholoba achates</i>
Cnidaria	Anthozoa	Sagartiidae	1	<i>Anthothoe sp.</i>
Cnidaria	Anthozoa	Sagartiidae	1	<i>Anthothoe chilensis</i>
Cnidaria	Anthozoa	Actiniidae	1	<i>Boloceropsis sp.</i>
Cnidaria	Anthozoa	Actiniidae	1	<i>Bunodactis octoradiata</i>
Cnidaria	Anthozoa	Clavulariidae	1	<i>Incrustatus comauensis</i>
Cnidaria	Anthozoa	Sagartiidae	1	<i>Actinothoe lobata</i>
Cnidaria	Hydrozoa	Campanulariidae	1	<i>Obelia geniculata</i>
Cnidaria	Hydrozoa	Symplectoscyphidae	1	<i>Symplectoscyphus subdichotomous</i>
Echinodermata	Asteroidea	Asteriidae	4	<i>Anasterias antarctica</i>
Echinodermata	Asteroidea	Stichasteridae	4	<i>Cosmasterias lurida</i>
Echinodermata	Asteroidea	Ganeriidae	4	<i>Cycethra verrucosa</i>
Echinodermata	Asteroidea	Echinasteridae	4	<i>Henricia obesa</i>
Echinodermata	Asteroidea	Echinasteridae	4	<i>Henricia studeri</i>
Echinodermata	Asteroidea	Heliasteridae	4	<i>Labidiaster radius</i>
Echinodermata	Asteroidea	Odontasteridae	4	<i>Odontaster penicillatus</i>
Echinodermata	Asteroidea	Asterinidae	4	<i>Asterina fimbriata</i>
Echinodermata	Asteroidea	Poraniidae	4	<i>Glabraster antarctica</i>
Echinodermata	Asteroidea	Poraniidae	4	<i>Poraniopsis echinaster</i>
Echinodermata	Asteroidea	Stichasteridae	4	<i>Stichaster striatus</i>
Echinodermata	Echinoidea	Parechinidae	3	<i>Loxechinus albus</i>
Echinodermata	Echinoidea	Arbaciidae	3	<i>Arbacia dufresnii</i>

S1 Table. Continued.

Phylum	Class to Infraclass	Order to Family	Func. Grp	Taxa
Echinodermata	Echinoidea	Cidaridae	4	<i>Austrocidaris canaliculata</i>
Echinodermata	Echinoidea	Temnopleuridae	3	<i>Pseudechinus magellanicus</i>
Echinodermata	Holothuroidea	Cucumariidae	1	<i>Cladodactyla crocea croceoides</i>
Echinodermata	Holothuroidea	Cucumariidae	1	<i>Pseudocnus dubius meloninus</i>
Echinodermata	Ophiuroidea	Ophiactidae	6	<i>Ophiactis asperula</i>
Echinodermata	Ophiuroidea	Ophiomyxidae	6	<i>Ophiomyxa vivipara</i>
Echinodermata	Ophiuroidea	Ophiuridae	6	<i>Ophiura (Ophiuroglypha) lymani</i>
Mollusca	Bivalvia	Gaimardiidae	2	<i>Gaimardia trapesina</i>
Mollusca	Bivalvia	Pectinidae	2	<i>Zygochlamys patagonica</i>
Mollusca	Gastropoda	Volutidae	4	<i>Adelomelon ancilla</i>
Mollusca	Gastropoda	Dorididae	4	<i>Doris fontainii</i>
Mollusca	Gastropoda	Ranellidae	4	<i>Argobuccinum pustulosum</i>
Mollusca	Gastropoda	Muricidae	4	<i>Concholepas concholepas</i>
Mollusca	Gastropoda	Discodorididae	4	<i>Diaulula hispida</i>
Mollusca	Gastropoda	Discodorididae	4	<i>Diaulula punctuolata</i>
Mollusca	Gastropoda	Fissurellidae	3	<i>Fissurella pict/oriens</i>
Mollusca	Gastropoda	Fissurellidae	3	<i>Fissurellidea patagonica</i>
Mollusca	Gastropoda	Ranellidae	4	<i>Fusitriton magellanicus</i>
Mollusca	Gastropoda	Calliostomatidae	3	<i>Margarella violacea</i>
Mollusca	Gastropoda	Nacellidae	3	<i>Nacella deaurata/magellanica</i>
Mollusca	Gastropoda	Nacellidae	3	<i>Nacella mytilina</i>
Mollusca	Gastropoda	Naticidae	6	<i>Naticarius</i> sp.
Mollusca	Gastropoda	Buccinidae	4	<i>Pareuthria fuscata</i>
Mollusca	Gastropoda	Tegulidae	3	<i>Tegula atra</i>
Mollusca	Gastropoda	Polyceridae	4	<i>Thecacera darwini</i>
Mollusca	Gastropoda	Tritoniidae	4	<i>Tritonia challengeriana</i>
Mollusca	Gastropoda	Muricidae	4	<i>Trophon geversianus</i>
Mollusca	Gastropoda	Muricidae	4	<i>Trophon plicatus</i>
Mollusca	Gastropoda	Chromodorididae	4	<i>Tyrinna delicata</i>

S1 Table. Continued.

Phylum	Class to Infraclass	Order to Family	Func. Grp	Taxa
Mollusca	Gastropoda		4	Unidentified opisthobranchia
Mollusca	Gastropoda	Muricidae	4	<i>Xymenopsis muriciformis</i>
Mollusca	Polyplacophora	Callochitonidae	3	<i>Callochiton puniceus</i>
Mollusca	Polyplacophora	Leptochitonidae	3	<i>Leptochiton cf. medinae</i>
Mollusca	Polyplacophora	Chitonidae	3	<i>Tonicia atrata</i>
Mollusca	Polyplacophora	Chitonidae	3	<i>Tonicia chilensis</i>
Mollusca	Polyplacophora	Chitonidae	3	<i>Tonicia smithii</i>
Mollusca	Polyplacophora	Chitonidae	3	<i>Chiton boweni</i>
Mollusca	Polyplacophora	Mopaliidae	3	<i>Plaxiphora aurata</i>
Nemertea	Anopla	Valenciniidae	4	<i>Baseodiscus aureus</i>
Porifera	Calcarea	Sycettidae	2	<i>Sycon</i> spp.
Porifera	Calcarea	Clathrinidae	2	<i>Clathrina cf. fjordica</i>
Porifera	Calcarea	Leucaltidae	2	<i>Leucettusa nuda</i>
Porifera	Demospongiae	Niphatidae	2	<i>Amphimedon maresi</i>
Porifera	Demospongiae	Clionidae	2	<i>Cliona chilensis</i>
Porifera	Demospongiae	Dysideidae	2	<i>Dysidea</i> sp.
Porifera	Demospongiae	Chalinidae	2	<i>Haliclona cf. porcelana</i>
Porifera	Demospongiae	Hymedesmiidae	2	<i>Hemimycale</i> sp.
Porifera	Demospongiae	Mycalidae	2	<i>Mycale (Aegogropila) magellanica</i>
Porifera	Demospongiae	Hymedesmiidae	2	<i>Phorbas</i> sp.
Porifera	Demospongiae	Polymastiidae	2	<i>Polymastia</i> sp.
Porifera	Demospongiae	Tethyidae	2	<i>Tethya papillosa</i>
Porifera	Demospongiae	?	2	Unid. yellow sponge
Porifera	Demospongiae	Chondrosiidae	2	Unid. <i>Chondrosia</i> -like
Porifera	Demospongiae	?	2	Unid. encrusting black sponge
Porifera	Demospongiae	Scopalinidae	2	<i>Scopalina</i> sp.
Porifera	Demospongiae	Mycalidae	2	<i>Mycale</i> sp.
Porifera			2	Unid. grey sponge

S2 Table. Taxa observed on deep sea Drop-cams.

Phylum	Class	Order	Family	Taxa	Common name	Freq (%)	MaxN	Max			
Porifera					Sponge	75		0.3			
Bryozoa	Gymnolaemata	Cheilostomatida	Microporellidae	<i>Microporella hyadesi</i>	Bryozoan	8.3	0.2				
					Bryozoan	16.7	0.4				
					Bryozoan			0.1			
Cnidaria	Stenolaemata	Cyclostomatida	Entalophoridae	<i>Entalophora sp.</i>	Bryozoan	16.7	1.7	0.2			
					Anthozoa	Actiniaria	Actinostolidae	<i>Paranthus niveus</i>	Anemone	8.3	0.4
	Hydrozoa	Anthoathecata	Stylasteridae	<i>Tethocyathus endesa</i>	Alcyonacea	Primnoidae	Octocoral	16.7	3.9		
					Scleractinia	Caryophylliidae	<i>Tethocyathus endesa</i>	Coral	8.3		0.05
					<i>Errina antarctica</i>	Hydrocoral	8.3	0.2			
					Hydrocoral	16.7	1				
Arthropoda	Malacostraca	Amphipoda			Amphipod	8.3	5				
Mollusca	Bivalvia	Nuculida	Nuculidae	<i>Nucula pisum</i>	Clam	8.3	0.4				
	Cephalopoda	Octopoda	Octopodidae	<i>Robsonella fontaniana</i>	Octopus	8.3	0.1				
	Gastropoda	Neogastropoda	Volutidae	<i>Adelomelon ancilla</i>	Sea snail	8.3	0.1				
				<i>Odontocymbiola magellanica</i>	Sea snail	8.3	0.1				
Echinodermata	Asteroidea	Forcipulatida	Stichasteridae	<i>Cosmasterias lurida</i>	Sea star	25	0.3				
		Spinulosida	Echinasteridae	<i>Henricia obesa</i>	Sea star	8.3	0.3				
		Valvatida	Ganeriidae	<i>Cycethra verrucosa</i>	Sea star	8.3	0.7				
		Velatida	Pterasteridae	<i>Pteraster gibber</i>	Slime star	8.3	0.3				
	Echinoidea	Arbacioida	Arbaciidae	<i>Arbacia dufresnii</i>	Sea urchin	8.3	0.3				
		Cidaroida	Cidaridae	<i>Austrocidaris canaliculata</i>	Sea urchin	8.3	0.1				
	Ophiuroidea	Phrynophiurida	Gorgonocephalidae	<i>Gorgonocephalus chilensis</i>	Basket star	8.3	0.1				
	Chordata	Actinopterygii	Clupeiformes	Clupeidae	<i>Sprattus fuegensis</i>	Fueguian sprat	25	5.7			
			Perciformes	Bovichtidae	<i>Cottoperca trigloides</i>	Thornfish	16.7	0.3			
				Nototheniidae	<i>Patagonotothen cornucola</i>	Cod icefishes	41.7	1			
Chondrichthyes		Scorpaeniformes	Sebastidae	<i>Sebastes oculatus</i>	Patagonian redfish	16.7	0.2				
		Carcharhiniformes	Scyliorhinidae	<i>Schroederichthys bivius</i>	Narrowmouth Catshark	8.3	0.1				
		Rajiformes	Arhynchobatidae	<i>Bathyraja magellanica</i>	Magellan skate	16.7	0.2				
		Myxini	Myxiniformes	Myxinidae	<i>Myxine australis</i>	Southern hagfish	50	1.2			

